AD-A086 227 NAVAL RESEARCH LAB WASHINGTON DC F/G 18/13
STRUCTURAL INTEGRITY OF WATER REACTOR PRESSURE BOUNDARY COMPONE--ETC(U)
AUG 80 F J LOSS
UNCLASSIFIED NRL-MR-4254 NRC-RES-79-103 NUREG-CR-1472 NL

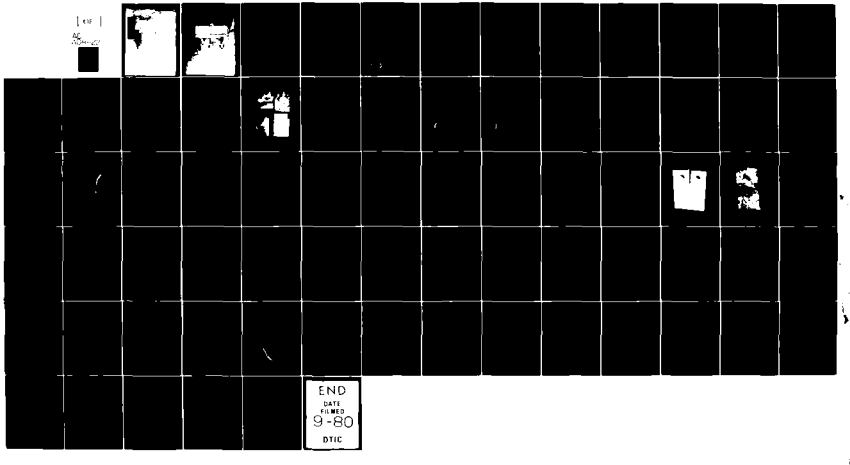

END
DATE FILMED
9-80
DTIC

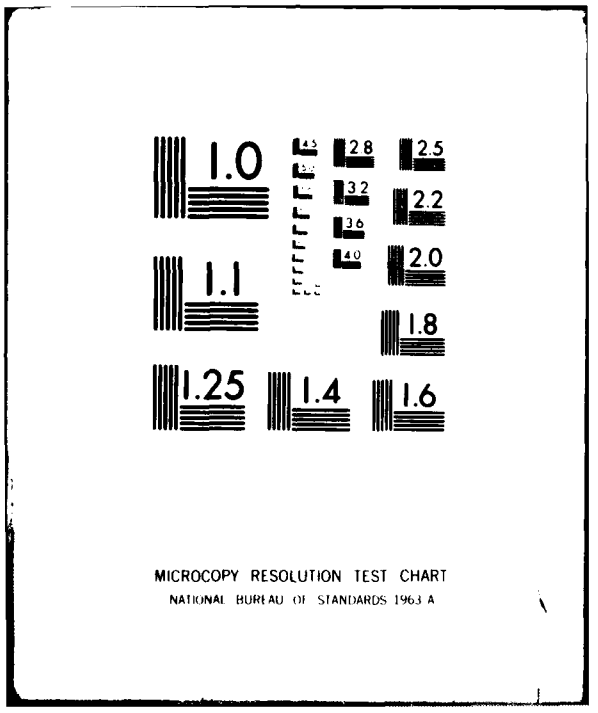
1.0
1.1
1.25
1.4
1.6
1.8
2.0
2.2
2.5
28
32
36
40
MICROCOPY RESOLUTION TEST CHART
NATIONAL BUREAU OF STANDARDS 1963 A

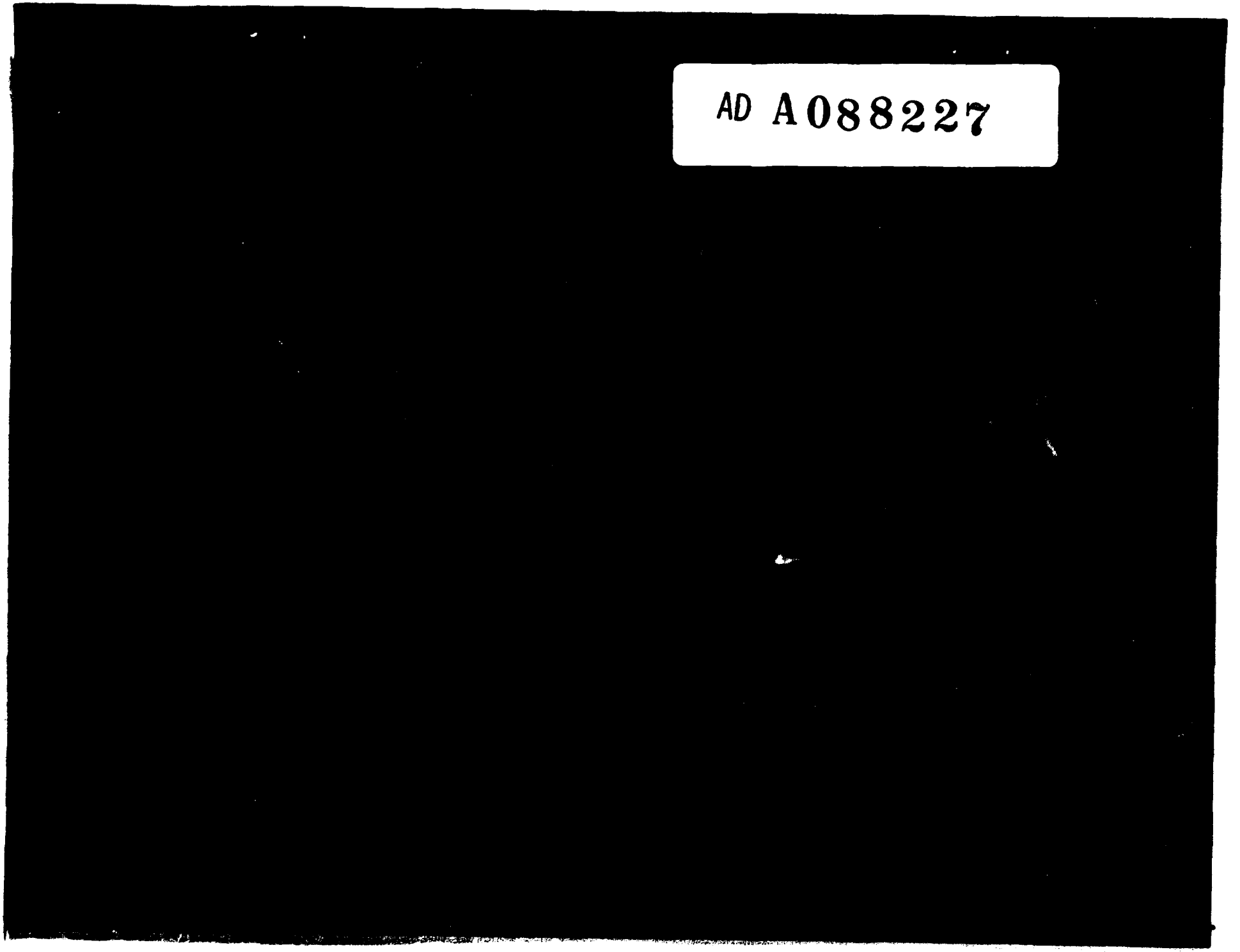

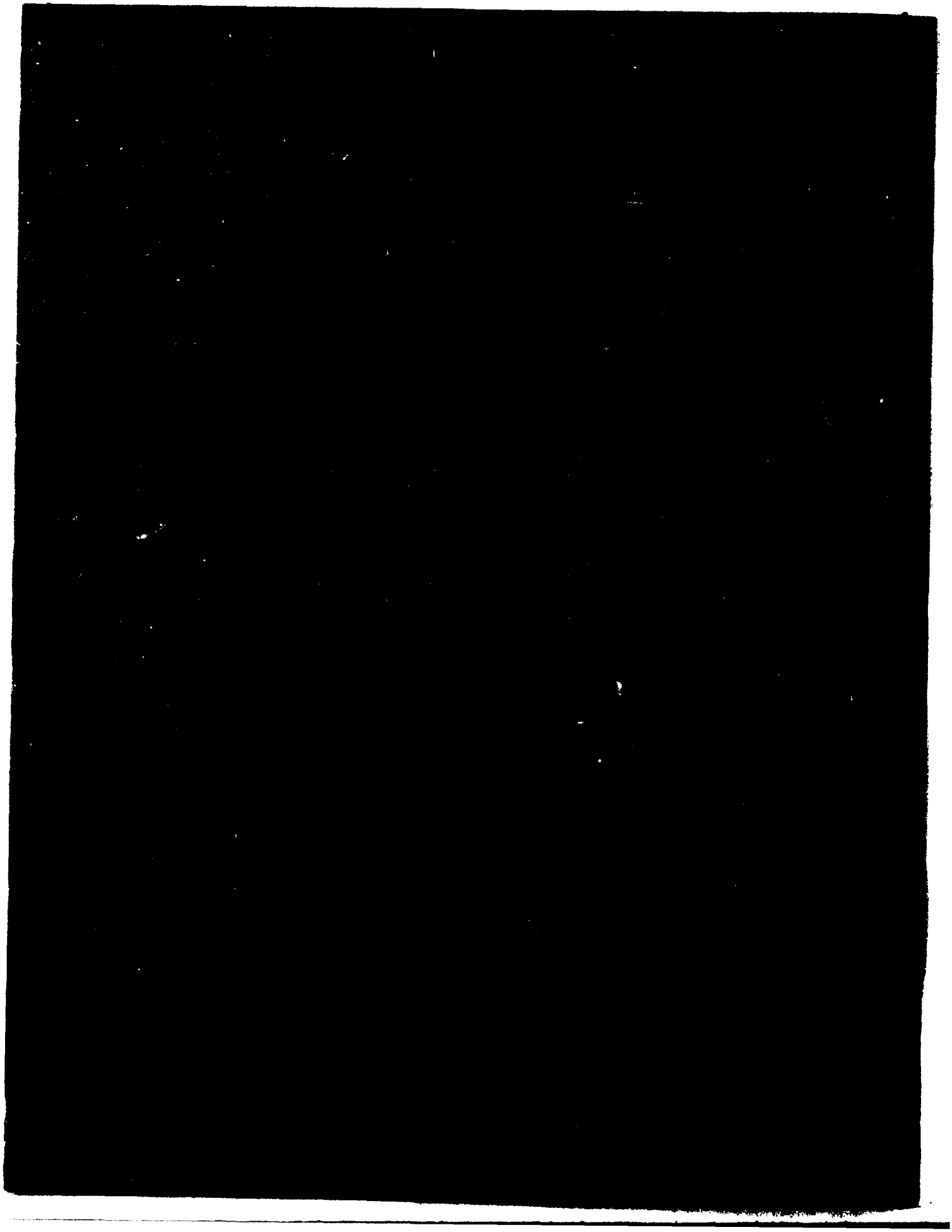

SECURITY CLASSIFICATION OF THIS PAGE *(When Data Entered)*

REPORT DOCUMENTATION PAGE

READ INSTRUCTIONS BEFORE COMPLETING FORM

1. REPORT NUMBER NUREG/CR-1472 NRL Memorandum Report 4254	2. GOVT ACCESSION NO. AD-A088
3. RECIPIENT'S CATALOG NUMBER 227	
4. TITLE *(and Subtitle)* STRUCTURAL INTEGRITY OF WATER REACTOR PRESSURE BOUNDARY COMPONENTS, QUARTERLY PROGRESS REPORT, JANUARY – MARCH 1980	5. TYPE OF REPORT & PERIOD COVERED Progress report on a continuing NRL problem. 6. PERFORMING ORG. REPORT NUMBER
7. AUTHOR(s) F. J. Loss, Editor	8. CONTRACT OR GRANT NUMBER(s) NRC-RES-79-103 FIN B5528 B&R 60191103
9. PERFORMING ORGANIZATION NAME AND ADDRESS Naval Research Laboratory Washington, D.C. 20375	10. PROGRAM ELEMENT, PROJECT, TASK AREA & WORK UNIT NUMBERS 63-1065-0-0
11. CONTROLLING OFFICE NAME AND ADDRESS U.S. Nuclear Regulatory Commission Division of Reactor Safety Research Washington, D.C. 20555	12. REPORT DATE August 1, 1980 13. NUMBER OF PAGES 71
14. MONITORING AGENCY NAME & ADDRESS*(if different from Controlling Office)*	15. SECURITY CLASS. *(of this report)* UNCLASSIFIED 15a. DECLASSIFICATION/DOWNGRADING SCHEDULE

16. DISTRIBUTION STATEMENT *(of this Report)*

Approved for public release; distribution unlimited.

17. DISTRIBUTION STATEMENT *(of the abstract entered in Block 20, if different from Report)*

18. SUPPLEMENTARY NOTES

Prepared for the U.S. Nuclear Regulatory Commission, Office of Nuclear Regulatory Research, Division of Reactor Safety Research under Interagency Agreement RES-79-103.

NRC Distribution Category R5 and AN.

19. KEY WORDS *(Continue on reverse side if necessary and identify by block number)*

A533-B submerged arc weld	Nuclear pressure vessel steels	Corrosion fatigue
Charpy V-test	Postirradiation recovery	Stress corrosion cracking
Fatigue crack propagation	Radiation sensitivity	
J-integral, R-curve	Single specimen compliance test	
Low upper shelf	Elastic-plastic fracture	

20. ABSTRACT *(Continue on reverse side if necessary and identify by block number)*

This report describes progress in a continuing program to characterize material properties performance with respect to structural integrity of light water reactor pressure boundary components. Progress under fracture mechanics describes J-R curve trends from a low shelf A302-B steel and includes a comparison of R curves by the multispecimen and single specimen compliance procedures. Fatigue crack growth rates are being determined for a variety of pressure vessel and piping steels in simulated nuclear coolant environments. Static load cracking in this environment has been observed in bolt-loaded specimens taken from weld heat-affected zones. Work in radiation sensitivity and postirradiation properties recovery has defined tensile property changes under cyclic annealing → next page

(Continues)

DD FORM 1 JAN 73 1473 EDITION OF 1 NOV 65 IS OBSOLETE
S/N 0102-LF-014-6601

SECURITY CLASSIFICATION OF THIS PAGE *(When Data Entered)*

20. Abstract (Continued)

and reirradiation treatments. Recent progress is described in radiation studies involving reactor vessel steels in a coordinated IAEA program. Also reported are notch ductility tests of reference steels of the NRC light water reactor, pressure vessel irradiation dosimetry program.

CONTENTS

ABSTRACT i

PREFACE iv

SUMMARY 1

RESEARCH PROGRESS 3

I. FRACTURE MECHANICS INVESTIGATIONS

A. J-R Curve Trends of A302-B Steel Having a Low Upper Shelf . 3

II. FATIGUE CRACK PROPAGATION IN LWR MATERIALS

A. Evaluation of Critical Factors in Crack Growth Rate Studies . 16

B. Corrosion Fatigue Crack Growth Behavior of Pressure Vessel Steels 37

III. RADIATION SENSITIVITY AND POSTIRRADIATION RECOVERY

A. IAR Program Investigations of Charpy-V Notch Ductility and Tensile Property Trends With Cyclic Postirradiation Annealing and Reirradiation 50

B. Evaluation and Comparison of IAEA Coordinated Program Steels and Welds with 288°C Irradiation 54

C. Mechanical Properties of LWR-PVI Surveillance Dosimetry Program Steels 60

REFERENCES 66

PREFACE

The goal of this program is to characterize materials behavior in relation to structural safety and reliability of pressure boundary components for light water reactors. Specific objectives include developing an understanding of elastic-plastic fracture and corrosion fatigue crack propagation phenomena in terms of continuum mechanics, metallurgical variables, and neutron irradiation. Emphasis is placed on identifying metallurgical factors responsible for radiation embrittlement of steels and developing procedures for embrittlement relief, including guidelines for radiation resistant steels. The underlying objective is the interpretation of material properties performance to establish engineering criteria for structural reliability and long term operation. Current work is organized into three major tasks: (1) fracture mechanics investigations, (2) fatigue crack propagation in high-temperature, primary reactor water, and (3) radiation sensitivity and postirradiation properties recovery. A part of the corrosion fatigue tests in Task 2 is being performed under subcontract to the Westinghouse Electric Corporation. This work is being coordinated with on-going research of a similar nature at NRL to form a uniform program having common objectives.

This work is being performed at NRL by the Material Science and Technology Division, Thermostructural Materials Branch, F. J. Loss, program manager. NRC funding is provided by the Division of Reactor Safety Research, Metallurgy and Materials Research Branch, Milton Vagins, project manager.

STRUCTURAL INTEGRITY OF WATER REACTOR PRESSURE BOUNDARY COMPONENTS QUARTERLY PROGRESS REPORT, JAN-MAR 1980

SUMMARY

I. FRACTURE MECHANICS INVESTIGATIONS

A. J-R Curve Trends of A302-B Steel Having a Low Upper Shelf

An assessment of the elastic-plastic behavior of an A302-B reactor vessel steel having a low upper shelf toughness is presented in terms of the J-R curve and tearing modulus. Similarities and differences between the proposed ASTM multispecimen standard for J_{Ic} and the single specimen compliance procedure are highlighted. Experimental investigations have disclosed for the first time an unstable fracture phenomenon in a vessel steel of low toughness in which the crack extension in the specimen is driven in a ductile but uncontrolled manner by the compliance of the testing system. A size effect study with 1/2T- and 1T-CT specimens has shown that both specimens will produce similar R curves for this steel. This similarity suggests that the limitation of crack extension to 6 percent of the unbroken ligament to insure J dominance, is conservative. Consequently, it may be possible to project a broader interpretation of R curve results from small size specimens.

II. FATIGUE CRACK PROPAGATION IN LWR MATERIALS

A. Evaluation of Critical Factors in Cyclic Crack Growth Rate Studies

Fatigue crack growth rate (FCGR) data are presented for unirradiated and irradiated pressure vessel steels, tested according to the main matrix test plan. For load ratios of 0.2, and temperatures of 288°C, FCGR for both irradiated and unirradiated steels reside under the ASME Code default limit for surface cracks exposed to the reactor coolant environment. The data from irradiated specimens resides just slightly higher than comparable data from unirradiated specimens. Some details concerning refinements in test practice, data presentation, and an overview of combined NRL and Westinghouse progress on the main matrix test plan is also included in this section.

Manuscript submitted May 27, 1980.

B. Corrosion Fatigue Crack Growth Behavior of Pressure Vessel Steels

Testing is continuing on the matrix being executed jointly by Westinghouse and NRL to characterize weld and HAZ materials. Four specimens were completed during this report period, two weld and two HAZ specimens. Fatigue crack growth rate results were found to be equal or slower than those of base metal specimens tested under the same loading conditions.

Static load cracking has now occurred in all of the five bolt-loaded specimens taken from weld heat-affected zones. Two heat-affected zones are represented, one from a forging and the other from a plate material. No static cracking has occurred in base metal or weld specimens in over 34,000 hours in the environment when the initial precrack was placed in this material. However, cracking in the weld and plate did occur when the initial crack was placed in the HAZ.

III. RADIATION SENSITIVITY AND POSTIRRADIATION PROPERTIES RECOVERY

A. IAR Program Investigations of Charpy V-Notch Ductility and Tensile Property Trends With Cyclic Postirradiation Annealing and Reirradiation

A report compiling Charpy-V (C_v) test results from all IAR Program Phase 1 experiments has been developed for presentation to the 1980 ASTM Radiation Effects Symposium. New data include the results from individual irradiation capsules forming Experiment Series 3 and 4 and test results for tensile specimens included in these same capsules. In each case, the data demonstrate that property changes were less for material subjected to the intermediate annealing and reirradiation schedule than material irradiated without annealing.

B. Evaluation and Comparison of IAEA Coordinated Program Steels and Welds With 288°C Irradiation

Three steel materials supplied by France and one weld deposit supplied by the Federal Republic of Germany (FRG) to the IAEA Program on "Analysis of the Behavior of Advanced Reactor Pressure Vessel Steels Under Neutron Irradiation," have been evaluated for preirradiation Charpy-V notch ductility. With one exception (the forging produced in France), the materials showed relatively low brittle/ductile transition temperatures and high upper shelf energy levels.

C. Mechanical Properties of LWR-PVI Surveillance Dosimetry Program Steels

An NRL task, in connection with the NRC light water reactor, pressure vessel irradiation (LWR-PVI) surveillance dosimetry program, is the development of mechanical properties data for two reference steel plates (ASTM A302-B reference plate, HSST Program A533-B Plate 03). During this quarter, the Charpy-V notch ductility properties of the plates were determined for the particular plate sections involved in the irradiation studies. The current report also describes the specimen inventory provided by NRL to the full program, including specimens designated for experiments in the NRC pressure vessel mock-up known as the pool side facility (PSF).

RESEARCH PROGRESS

I. FRACTURE MECHANICS INVESTIGATIONS

A. J-R Curve Trends of A302-B Steel Having a Low Upper Shelf

F. J. Loss, B. H. Menke, R. A. Gray, Jr., V. Provenzano, and G. Angelino[1]

INTRODUCTION

The beltline region of nuclear pressure vessels suffers a progressive degradation in fracture toughness with increasing neutron fluence. Consequently, it is necessary to define the margin of safety against fracture for all operating conditions. This is especially true with steels of low upper shelf toughness, that is, steels whose Charpy-V notch energy falls below 68 J (50 ft-lb). While the steels used for current vessel construction are expected to exhibit a high fracture toughness throughout the service lifetime, certain steels, such as the Type A302-B used for early vessel construction, can exhibit a low upper shelf behavior.

The phenomenon of low shelf toughness presents some difficulty in assessing the margin of safety against fracture. Specifically, measurements of the plane strain initiation toughness, K_{Ic}, by ASTM standards do not exist at upper shelf level temperatures for reactor vessel steels because of their generally high toughness and the resultant large specimen sizes required for valid tests. Yet the current codes and standards used to assure fracture safety are based upon linear elastic fracture mechanics concepts (e.g., ASME Boiler and Pressure Vessel Code, Sec. III). Estimates of the upper shelf K_{Ic} level from small-specimen assessments using the J integral, i.e., K_{Jc} [1], have shown that this quantity will fall below 165 MPa $\sqrt{m}$ for steels of low shelf energy; the latter is considered as the level of toughness required to provide an adequate safety margin for normal operation and anticipated reactor transient conditions. Accident analyses may require a higher level of toughness.

The preceding facts have resulted in significant research programs being focused to characterize the elastic plastic behavior of nuclear structures. Of the approaches being actively pursued, the concept of plastic tearing instability [2] has received emphasis as a means to provide assurance against unstable fracture. The method relies upon the phenomenon of a J-R curve which exhibits an apparent increase in toughness with crack extension. This R curve behavior is of prime importance in that it forms the physical basis upon which to preclude unstable fracture for cases in which crack initiation must be assumed. The tearing instability approach has been successfully demonstrated in the laboratory [2], but it still requires a structural verification. Likewise, the J-R curve behavior of pressure vessel steels of low toughness must be thoroughly established before

[1] Centro Informazioni Studi Esperienze, Milan, Italy.

the adequacy of the tearing instability concept can be assessed for this application.

The present investigation characterizes the elastic plastic toughness of an A302-B steel plate in terms of the J-R curve. This plate was produced to specifications used for older reactor vessels and has a Charpy-V (C_v) upper shelf energy of 68 J. Emphasis is placed on the single specimen compliance (SSC) procedure for R-curve measurement [3]. This method is contrasted with the multiple specimen procedure defined in the proposed ASTM standard for J_{Ic}. Also, in order to define possible size effects which could cloud structural interpretations made with small-size specimens used in reactor surveillance programs (e.g., 1/2T-CT specimens), a comparison is made between R curves developed with 1T-CT and 1/2T-CT specimens.

This program is the result of a cooperative effort between NRL and CISE (Centro Informazioni Studi Esperienze) [4]. Both laboratories investigated the A302-B steel with 1/2T- and 1T-CT specimens; NRL also conducted limited tests with a 10 mm thick, notched-bend specimen. The investigation by CISE emphasized the multiple specimen R-curve approach; NRL emphasis was on the SSC procedure as it is being developed for hot-cell testing of irradiated materials.

MULTIPLE SPECIMEN R-CURVE PROCEDURE

All specimens were cut from a 150 mm thick A302-B plate (Code V50) in the weak (TL) orientation. The mechanical properties of this plate are described in Ref. 5. Specimens were machined and precracked in accordance with ASTM E-399 to a crack length-to-width ratio (a/W) of 0.5. With the CT specimens, the notch geometry was modified slightly to permit the use of integrally-machined knife edges for the measurement of load-line displacement with a clip gage. The R curves were defined by sets of 4 to 6 specimens, with each specimen being loaded to a different load-line displacement. The final crack extension was marked by heat tinting. With the CT specimens at CISE the crack extension was measured at 10 to 15 thickness positions which, in turn, were used to map the crack profile. The average crack extension was obtained from the integrated area of the crack-extension profile. With the CT specimens and 10 mm bend specimens characterized by NRL, the average crack extension was computed from nine equally spaced measurements along the crack front; the measurements at the specimen surfaces were averaged as recommened by ASTM E-24. For the bend specimens, the load-line displacement was determined by means of ram travel, accounting for the elastic deflections of the ram and specimen loading fixture.

The J integral values were computed from the relationship:

$$J = \alpha_1 \frac{2A}{Bb_o} + \alpha_2 \frac{P\delta}{Bb_o} \qquad (1)$$

where α_1 and α_2 are the Merkle-Corten coefficients [6] which account for the tension component of the loading in the CT specimens, A is the area of the load vs load-line displacement record, B is the specimen thickness, b_o is the original unbroken ligament, P is the final load, and δ is the corresponding final load-line displacement.

The R curve is approximated by a least squares fit to the data between the 0.15 mm exclusion line and a parallel line at 1.5 mm crack extension as illustrated in Fig. 1. The J_{Ic} point is defined by the intersection of the R curve with the blunting line. The latter quantity is defined as $\Delta a = J/2\sigma_f$ where Δa is the crack extension and σ_f is a flow stress taken as the mean of the yield and ultimate strengths. The tearing modulus T_{Avg}

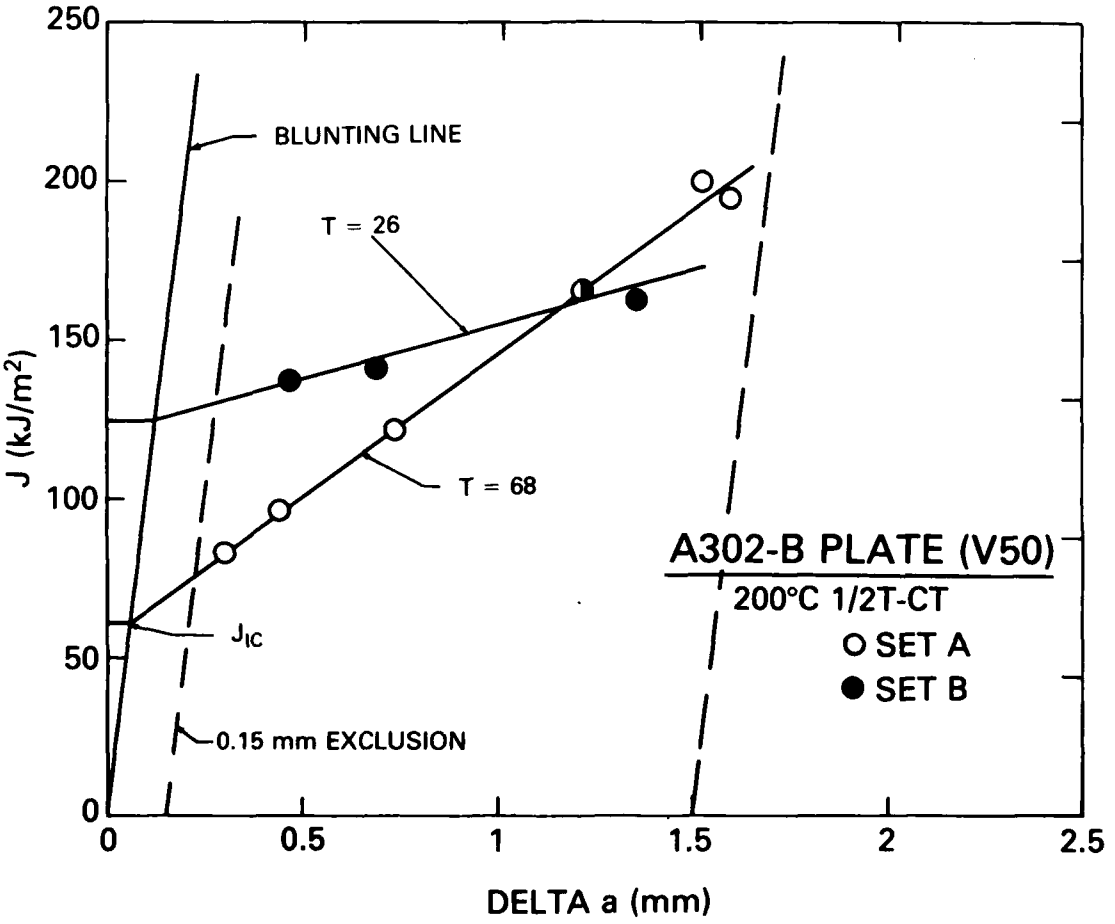

Fig. 1 — Multiple-specimen method for J_{Ic} determination illustrating the observed scatter

as used here is an average value computed as follows [2]:

$$T_{Avg} = \frac{dJ}{da} \frac{E}{\sigma_f 2} \quad (2)$$

where dJ/da is the average slope of the R curve and E is Young's modulus.

MULTISPECIMEN METHOD RESULTS

Figure 1 illustrates the observed scatter in J_{Ic} and T_{Avg} which can result with the multispecimen method. For two sets of data from 1/2T-CT specimens taken from the A302-B steel plate, this plot shows a 2:1 variation in J_{Ic} and a 2.6:1 variation in T_{Avg}. On the other hand, the results of two additional data sets (Fig. 2) exhibit little scatter and clearly indicate the curvature in the R curve.

When all of the 1/2T-CT data are plotted together (Fig. 3), the nonlinearity in the R curve is evident in spite of the data scatter. From this figure it is concluded that the plate exhibits no toughness trends as a function of thickness location. In addition, a difference in testing temperature, from 200 to 288°C has shown no significant effect. Note, however, that the results from 1T-CT tests at both test temperatures reside at the lower extreme and partially out of the 1/2T-CT scatterband. While these results suggest a small size effect between 1/2T-CT and 1T-CT specimens, it is felt that insufficient data exist to reliably draw such a conclusion in view of the scatterband.

Figure 4 compares the results of the 10 mm bend specimens tested by NRL with the 1/2T-CT scatterband (Fig. 3) defined by specimens tested by CISE. While the 10 mm specimens exhibit a larger scatter than do the 1/2T-CT specimens, it generally appears that the different specimen types tested by the two laboratories have defined the same R-curve behavior. When account is taken of the single 1/2T-CT data point in Fig. 3 which did not lie within the constructed boundary of the scatter, the scatterband from the two specimen types is identical.

Table 1 lists the J_{Ic} and T_{Avg} values produced by the multispecimen procedure using a least squares fit of the data. Also listed are the K_{Jc} values computed from the relationship:

$$K_{Jc} = \left[\frac{E J_{Ic}}{1 - \nu^2} \right]^{1/2} \quad (3)$$

where ν is Poisson's ratio. The 1/2T-CT vs the 10 mm bend specimens exhibit only a small (12%) variation in J_{Ic} and T_{Avg}. Therefore it is concluded that both specimen types are in substantial agreement. The corresponding values of J_{Ic} and T_{Avg} measured with the 1T-CT specimen are somewhat lower. However, this is believed to result, in part, from an insufficient quantity of data.

An alternative procedure for J_{Ic} was devised by NRL [1] and applied to the 1/2T-CT and 10-mm bend data by constructing a curved R curve as the average of the scatterband from each specimen type. As seen in the table, these values are essentially identical to those of the multispecimen procedure.

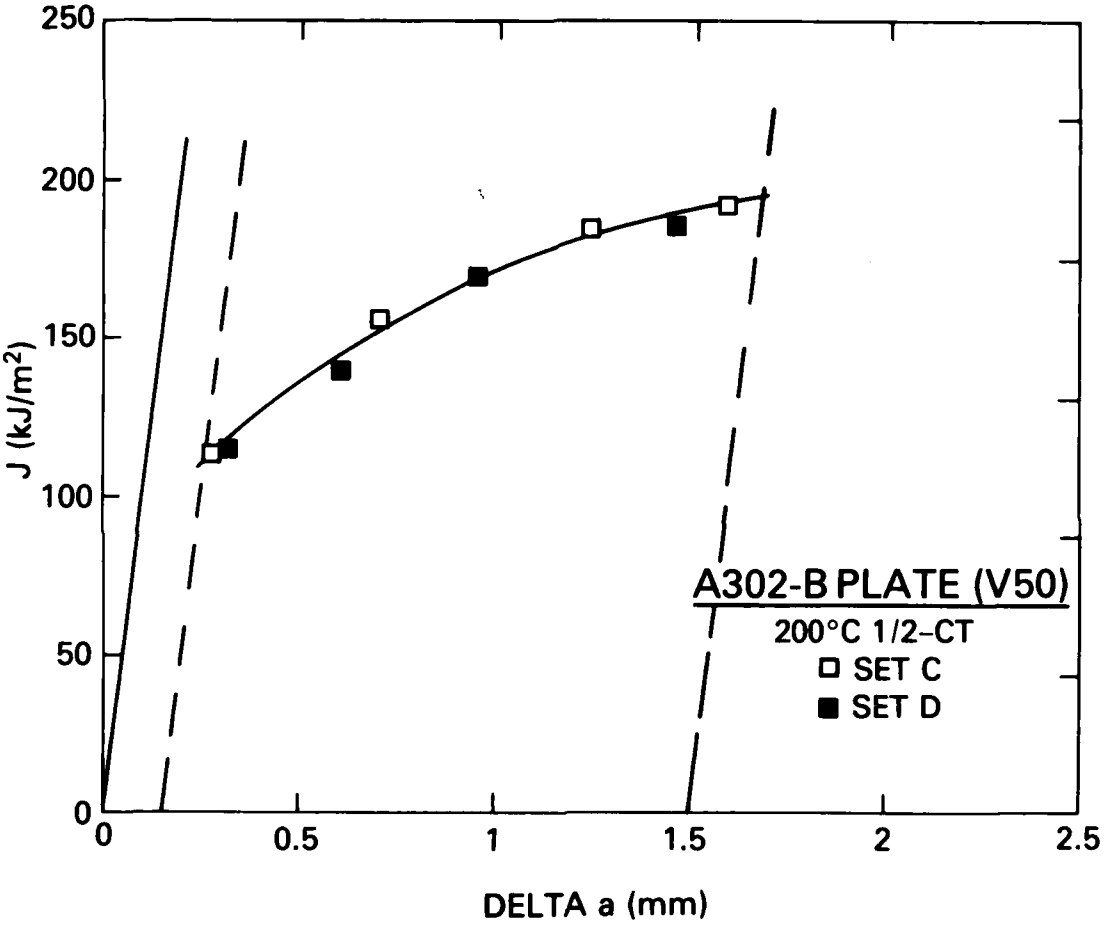

Fig. 2 — Nonlinear R curve described by multiple specimen tests

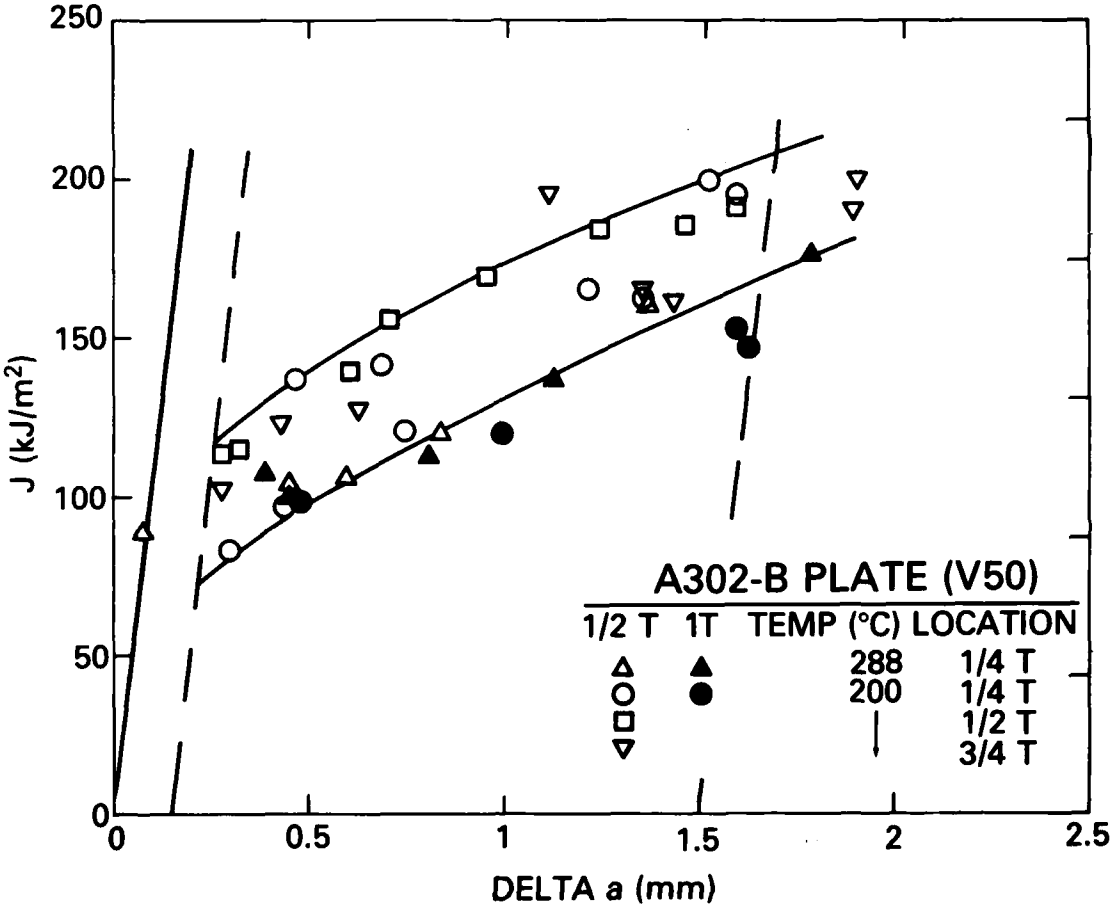

Fig. 3 — Summary of multispecimen results with 1/2T- and 1T-CT specimens

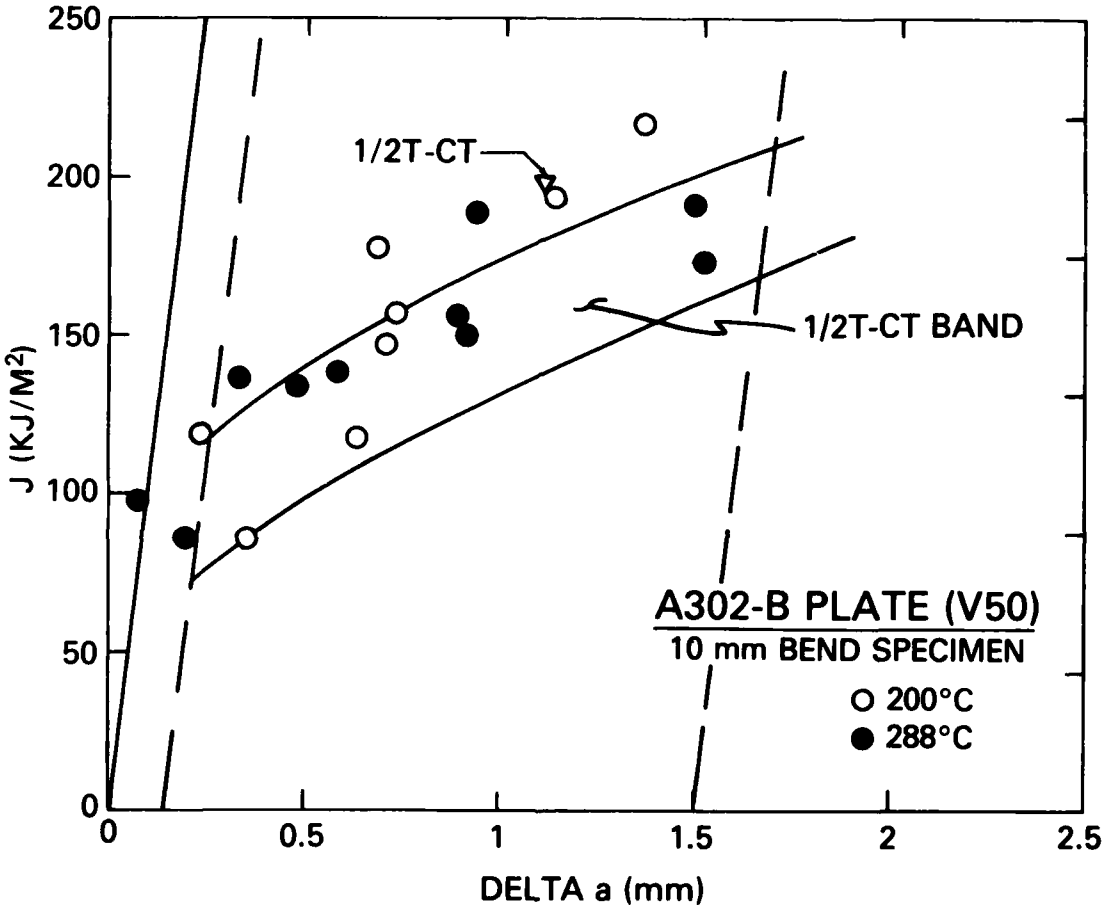

Fig. 4 — Summary of multispecimen results with 10 mm specimen

Table 1 - Toughness of A302-B Steel
With Multiple Specimen Tests at 200°C and 288°C

Specimen	J_{Ic} (kJ/m^2) Multispecimen	Alternative	K_{Ic} (MPa$\sqrt{m}$)	T_{Avg}
1/2T-CT	95	95	143	47
10 mm Bend	105	108	150	53
1T-CT	82	-	133	36

FRACTURE MORPHOLOGY

Unlike some A533-B steels of high toughness, the A302-B steel investigated here exhibited an extremely non-uniform metallurgical structure as illustrated in Fig. 5a,b. This non-uniformity is believed to result from non-metallic inclusions such as MnS which have been observed fractographically [7] and which contribute to the low toughness. The inclusion particles give rise to longitudinal bands elongated in the rolling direction. This results in the woody (fibrous) appearance of the fracture surface (Fig. 5a). The crack-front irregularity presents difficulty with the optical measurement of the crack extension and possibly accounts for some of the observed scatter in the R-curve data. The fracture surface of the A302-B steel is contrasted with that of an A533-B weld deposit (Code V86) in Fig. 5c,d. The texture of the latter is much more uniform and presents no problem in the optical measurements.

With the A302-B steel it has also been observed that areas of unbroken ligament remain within the heat-tinted area of the final crack extension. This is illustrated in Fig. 5b by the small area which failed in a cleavage mode when the specimen was broken apart at low temperature. This phenomenon suggests that the optical measurement of the crack extension profile may not be an accurate means of characterizing the physical behavior. This non-uniform crack extension was not observed with other A533-B steels investigated by NRL [1].

The crack front typically exhibits a tunneled shape (Fig. 5a) which results from the lack of mechanical constraint at the free surfaces. The latter permits plastic deformation at these locations at the expense of crack extension. There is disagreement as to whether this tunneling is representative of the crack front behavior of large cracks in a structure. Nevertheless, crack-front tunneling does result in a three-dimensional effect which may not be properly accounted for by the two-dimensional form of the J integral. It has been shown that side grooves in the specimens will eliminate the tunneling [1]. An example of this is illustrated in Fig. 5c.

With the SSC technique a severe tunneling of the crack front produces errors in the predicted crack extension. This inconsistency between the crack length predictions vs optical measurements has been verified experimentally by NRL investigators using specimens having a machined-tunneled shape [1]. This observed difference is reasonable in that the theoretical compliance relationship [8] used with the SSC technique to predict crack extension was derived on the basis of a straight crack-front extension. For this reason all of the SSC tests were conducted with specimens having 25 percent side grooves in order to eliminate the tunneling. Once a straight crack extension is assured, the SSC method can predict the optically-measured crack front to a high precision. However, in the case of the A302-B steel, the additional factor of a non-uniform crack front will cause the SSC technique to predict a somewhat shorter crack than that

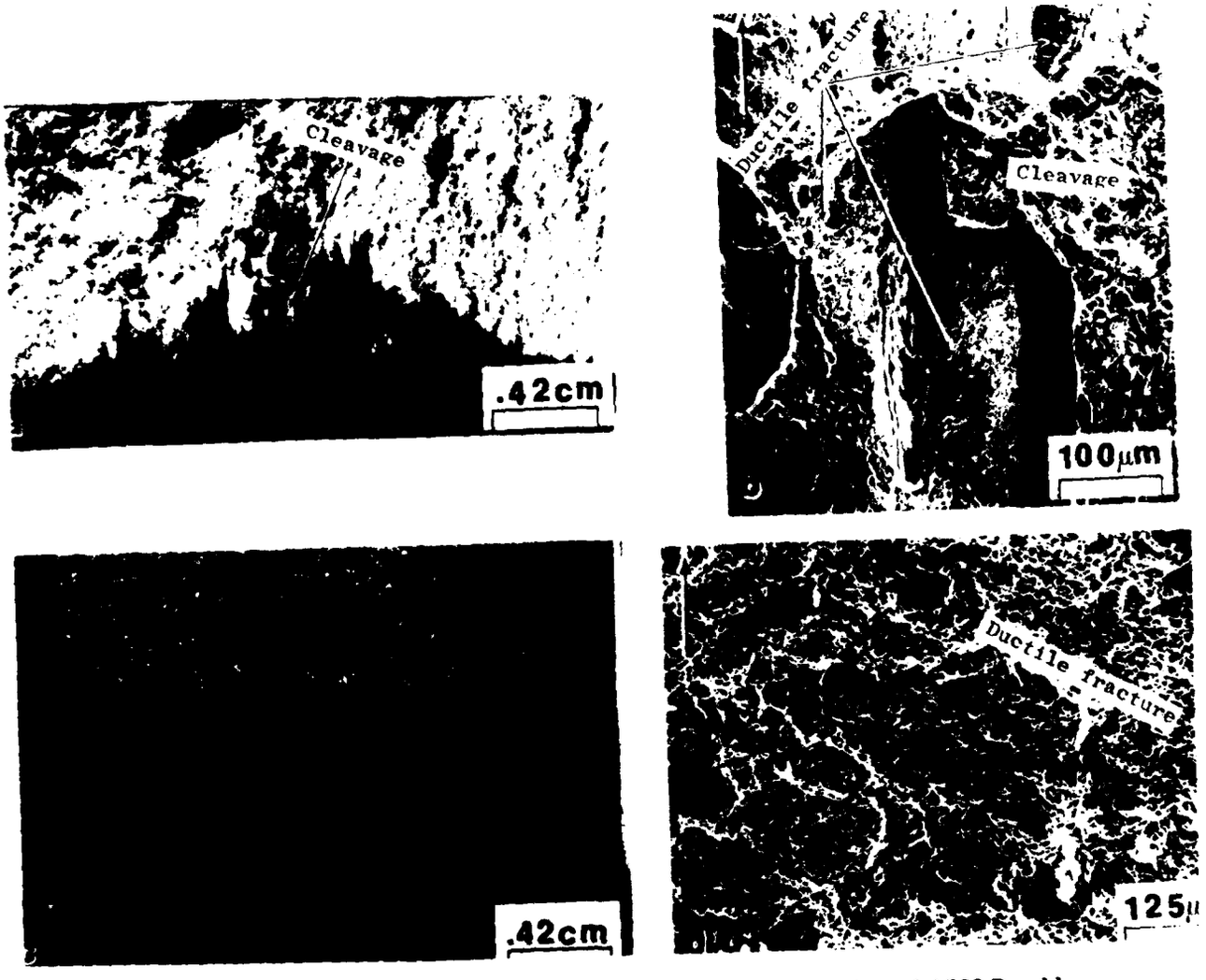

Fig. 5 — Fracture surface of 1T-CT specimens of A302-B steel (5a,b) and A533-B weld deposit (5c,d). The specimen in 5c has been side grooved by 20% to eliminate crack-front tunneling observed in 5a.

determined optically, even though the average crack front is straight. This behavior is attributed to the unbroken ligaments described above. These ligaments will increase the specimen stiffness and thereby result in a lower compliance (i.e., shorter crack length). With this type of behavior it is felt that the compliance method predicts the effective crack extension which would be associated with a structural prototype. For this reason, we consider the compliance-predicted value of crack extension as more significant than that measured by optical means.

SINGLE SPECIMEN COMPLIANCE RESULTS

The SSC method developed by NRL is described in Ref. [1]. In brief, this procedure treats the R curve as a nonlinear phenomenon which can be adequately described for small values of crack extension (Δa) by a power function having the form $J = C\Delta a^n$, where C and n are empirical constants. Because of this nonlinear behavior, an alternative definition for J_{Ic} has been proposed [1] as contrasted with the proposed ASTM J_{Ic} standard.

Figure 6 presents R curves for two steels determined by the SSC technique. A comparison is made between the trends exhibited by smooth specimens vs those from side-grooved specimens. With the latter the net thickness B_N is used in Eq. (1) to compute J. This is an approximation since an exact relationship for J does not exist for a side-grooved specimen. The lowest curve represents the average of five 1T-CT specimens having 25 percent side grooves which were cut from the A302-B plate. These data exhibit little scatter and a J_{Ic} of 73 kJ/m^2 was determined by the NRL alternative procedure. (The corresponding value of K_{Jc} is 125 MPa$\sqrt{m}$). This value is below the range of 82 to 105 kJ/m^2 defined by the smooth specimens (Table 1). For these same data, an average T of 22 was computed from the R curve between the 0.15 mm exclusion line and the parallel line at 1.5 mm crack extension. This quantity is a factor of two below that exhibited by the smooth specimens.

A 1/2T-CT specimen, also having 25 percent side grooves, was cut from the broken half of one of the 1T-CT specimens tested with the SSC method. The R curve from this specimen lies within the narrow scatterband of the 1T-CT data in Fig. 6. Since this specimen should be metallurgically identical with that of the 1T-CT specimen this correspondence reinforces the conclusion drawn earlier that there is no distinguishable size effect in the R curves between 1/2T-CT and 1T-CT specimens for a steel of this low toughness level.

The preceding 1/2T- and 1T-CT specimens experienced crack extensions of 0.06 b and 0.12 b respectively. The fact that similar R curves were produced from these specimens is inconsistent with a theoretical projection [9]. The latter has concluded that a large crack extension (>6 percent b) will violate the so-called region of J dominance within which the strain field characterized by J is not substantially influenced by the magnitude of the crack extension. As a consequence of these observations, it may be possible to extend the R curve beyond the preceding limit and still retain its usefulness with respect to structural interpretations.

While there are currently no size requirements for valid R-curve tests, the proposed ASTM multispecimen procedure suggests that the thickness (B) and ligament (b) be greater than $\alpha J/\sigma_f$ where α is 25 at the J_{Ic} level and is 15 elsewhere. With this criterion a 1/2T-CT specimen can be loaded to initial and maximum J levels of 260 kJ/m^2 and 430 kJm^2, respectively, with the 10 mm bend specimens the corresponding limits are 200 kJ/m^2 and 340 kJ/m^2. It is seen that all of the data from the A302-B plate (Figs. 3 and 6) meet these criteria.

In Fig. 6 the 1/2T- and 1T-CT specimen data determined with the multispecimen method (Fig. 3) have produced an R curve scatterband which lies above the curve defined with the side-grooved, 1T-CT specimens. This result was expected and is attributed to the lower constraint offered by the smooth specimens. A similar comparison with an A533-B submerged arc weld deposit [1] is also illustrated in Fig. 6. In this case, the SSC method was used to characterize the smooth and also the 20 percent side-grooved specimens. With both materials the use of side grooves has reduced the average value of T by a factor of 1-2/3 to 2. Thus it appears that the lower R-curve behavior of the side-grooved A302-B specimens is due to a change in mechanical constraint produced by the side grooves and is not related to the test procedure (multispecimen vs SSC).

Figure 7 illustrates R curves for the A302-B steel at 23°C which were also determined by the SSC procedure. In comparison with the tests conducted at 200°C (Fig. 6), the scatterband is larger and of a size comparable to that exhibited by the 1/2T-CT specimens (Fig. 3). At 23°C the average J_{Ic} value of 97 kJ/m^2 is one-third higher than that determined at 200°C for the same type specimen. On the other hand, the average T of 40 is almost double that measured at 200°C, thereby indicating a significant effect of temperature on the tearing modulus. To test the specimen thickness dependence of the R curve at 23°C, a 1/2T-CT specimen was cut from the broken half of a 1T-CT specimen. As illustrated in Fig. 6, the result is an almost exact correspondence of the R curves from the two specimen sizes; this confirms the absence of a thickness dependence.

Unstable Fracture Behavior

A few of the 1/2T- and 1T-CT specimens tested at 200°C and 288°C exhibited small increments (< 1 mm) of unstable crack extension during which it was not possible to maintain a controlled deflection rate by the testing machine. These incidents were observed after the specimen had reached maximum load. Thereafter the unstable propagation occurred in a ductile manner and at a slower velocity compared with that normally associated with brittle (cleavage) fracture. This phenomenon was observed by both CISE and NRL and is the first known incidence of this type in the upper shelf region for nuclear steels.

From these observations it is concluded that the tearing modulus of the material, T_{MAT}, was exceeded by the applied T of the testing machine, T_{APPL}. Consequently, this suggests that a similar behavior can occur in the structure after suitable plastic deformation in a localized region surrounding the flaw. In the structure, however, the increment of unstable crack extension could be larger, depending on the compliance of the structure.

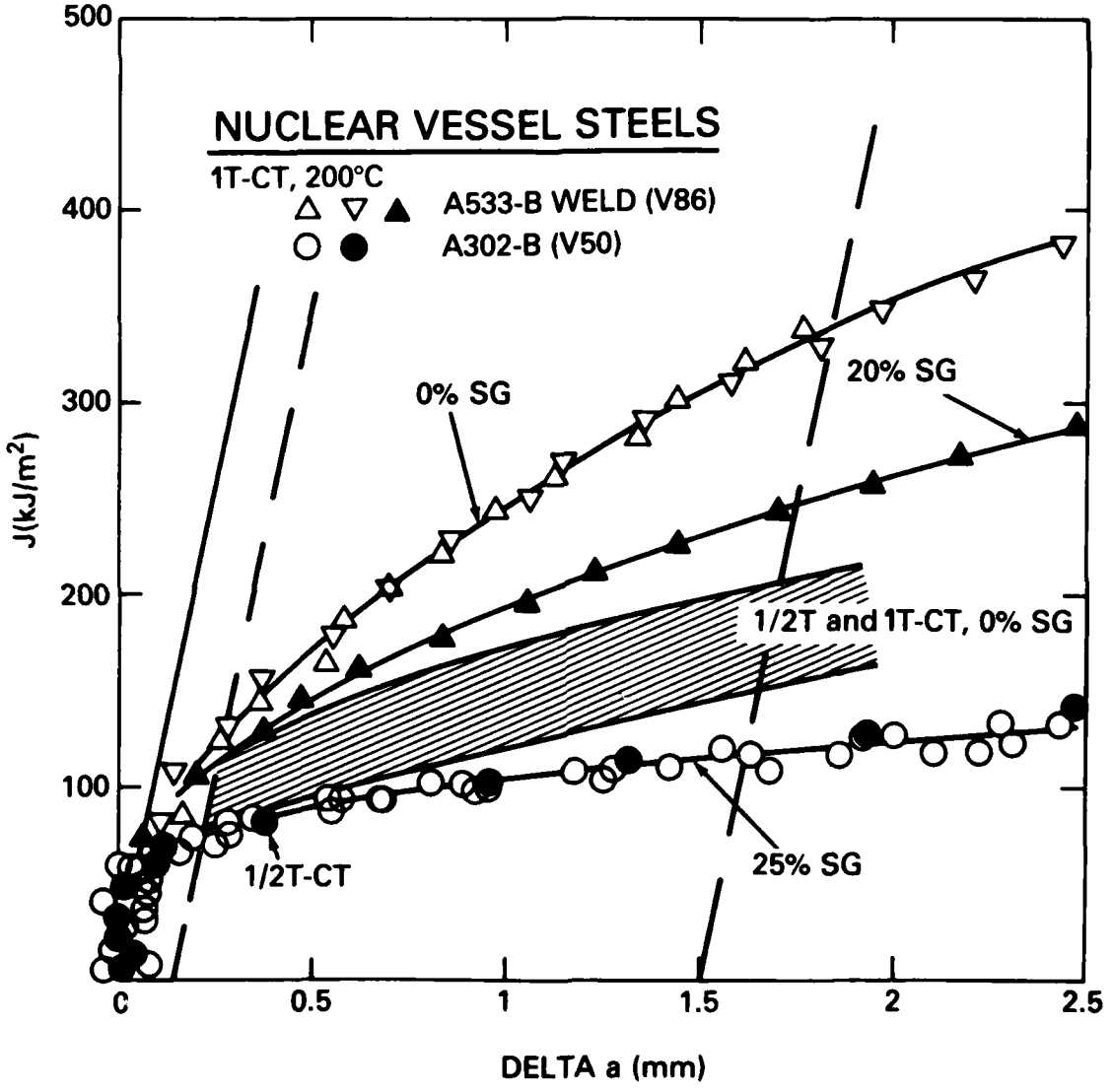

Fig. 6 — Comparison of R curve trends illustrating effects of side grooves

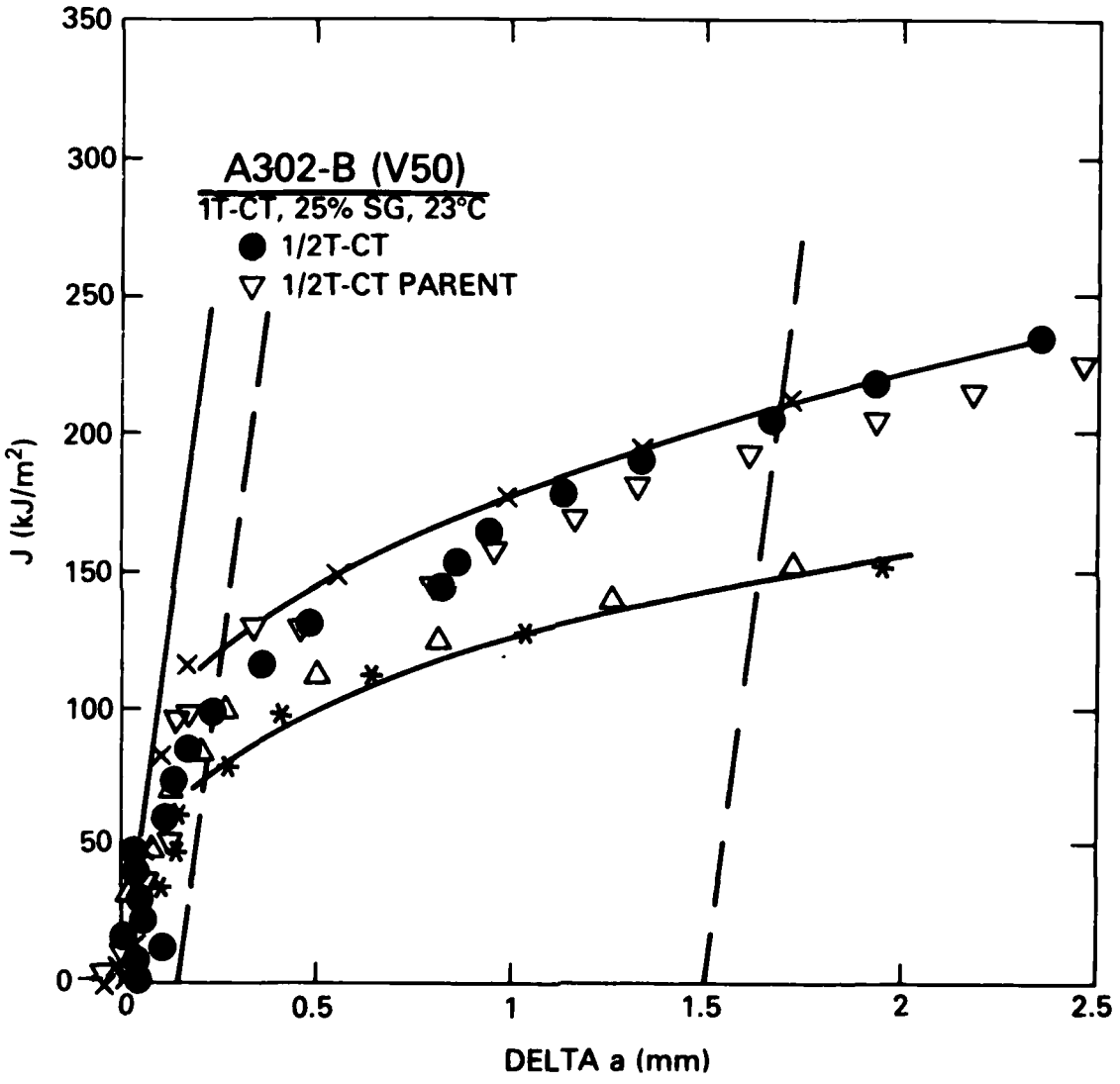

Fig. 7 — R curves for A302-B steel with the SSC procedure. Tests were conducted with 1T-CT specimens except as noted.

II. FATIGUE CRACK PROPAGATION IN LWR MATERIALS

A. Evaluation of Critical Factors in Crack Growth Rate Studies

W. H. Cullen, Jr., R. A. Taylor, H. E. Watson, and Wolfgang Rohrs[1]

BACKGROUND

The fatigue crack growth rate (FCGR) evaluation program at the NRL consists of several efforts which address specific topics of importance to nuclear reactor design, in-service inspection, and continued safe operation. Several tests are being carried out in an environment which simulates the PWR primary-loop, nuclear-core-coolant chemistry using waveforms which describe certain transients and operational changes in reactor pressure which may lead to subcritical extension of pre-existing flaws. These sub-programs are as follows:

a. Main Matrix Tests (Unirradiated) - a test plan aimed at evaluation of fatigue crack growth rates for several reactor pressure vessel steels and welds, including both fused weld metal and heat-affected zones. This program is conducted jointly by NRL and the Westinghouse Nuclear Energy Systems Division under a subcontract.

b. Main Matrix Tests (Irradiated) - this plan is actually a subset of the Main Matrix described above, and includes tests of selected specimens of the same materials as above, but irradiated to total fluences of 2 to 4 x 10^{19} n/cm^2 (>1 MeV). This testing is also carried out in the high-temperature, PWR water environment.

c. Piping Matrix - a test plan in which several piping materials are to be tested in the simulated PWR coolant environment. The waveforms and load ratios for these tests are similar to those selected for the Main Matrix tests.

d. Variable Amplitude/Variable Frequency Test Matrix - a test plan which is carried out in association with the cold leg integrity evaluation. Several tests of piping materials will be tested in the high-temperature, PWR water environment.

e. Supporting Tests - this includes a variety of tests to assist in the interpretation and application of the FCGR data from the above test plans. Additional FCGR tests at other temperatures, or with different loading waveforms, are underway, and some stress corrosion cracking tests are about to commence. Stress-corrosion cracking, fractographic, water chemistry and oxide film studies assist the interpretation of FCGR results, and have been key factors in the development of a model for hydrogen assisted crack growth in these materials in the simulated nuclear coolant environment [10].

TEST STATUS AND PROGRESS

The progress in each of these areas, during the past quarter, and a summary of expected developments is described in the following sections.

---

[1]Gesellschaft fur Reaktorsicherheit (GRS) mbH.

a. Main Matrix Tests (Unirradiated)

The status of main matrix tests, both completed and underway, is shown in Table 2. The items tested under the Westinghouse Subcontract are reported and discussed in a separate section. During this quarter, NRL has completed testing of one item from this matrix, has six tests underway, and at the end of this quarter, the NRL test status was that shown in Table 3.

Figure 8 shows fatigue crack growth data for A508-2 forging steel (specimen V82-5), tested with a 60 sec ramp/1 sec reset waveform, at 288°C. The dashed lines in this and other graphs of fatigue crack growth rate represent the air and water environment default lines from Appendix A of Section XI of the ASME Boiler and Pressure Vessel Code [11]. Figure 9 shows this same data set, together with earlier data for similar waveform and temperature conditions, but for different heat of A508. The earlier data sets reside near the ASME Section XI air default line and are part of a coherent set of results described in Ref. 10. The V82-5 specimen is obviously considerably more susceptible to fatigue crack growth in the high-temperature, pressurized water environment. The reasons for this are not yet clear. These are the first results for the V82 forging, but three other tests of this heat of material (including an irradiated 2T-CT specimen) are currently underway at the NRL, and the results from these may describe the trends which pertain to this particular heat. There is no reason to suspect that differences in the autoclave environment, or in mechanical test practice, could be responsible for the increase in growth rates, since this specimen was one of four specimens in a multispecimen daisy chain. Two of the other three specimens exhibited growth rates residing in the low category (W7-2C2 and Q342W2, described in the previous quarterly [12]) and the fourth specimen, of A106 piping steel (FOR-62), grew so little that the data cannot be meaningfully differentiated.

At the end of this quarterly reporting period, as shown in Table 2, 32 of a total of 63 main matrix tests have been jointly completed by the NRL and Westinghouse laboratories. In summary fashion, the matrix results basically fall in the categories, or regions, shown in Fig. 10. These regions were drawn after consideration of all of the high-temperature, pressurized, reactor-grade water fatigue crack growth data available in the literature. These regions are an attempt to represent the observed trends in a condensed, but still meaningful and comprehensive way; they do not, therefore, include data points which appear to be part of a test start-up, or other test-practice-related transient.

For the tests at the load ratio of 0.2, all of the 17 mHz sinewave results, from both laboratories, reside in the "HIGH, $R \leq 0.5$" category shown in Fig. 10. The 60 second ramp/reset results fall predominately in the "LOW" region, but among the 12 tests of this type so far completed, there have been some notable exceptions. A508-2 Specimen V82-5 (Fig. 8) falls in the higher growth rate category as does weld metal (Linde 124 flux) specimen C-7 ([13], Fig. 1). Specimen C-24-HAZ-1 ([13], Fig. 3), a heat-affected zone in A533B produced by a weld with Linde 124 flux also seems to reside in the high growth rate category. Other 60 sec. ramp/reset results from these, or similar materials fall in the low growth rate category. According to the previously proposed model for hydrogen assisted fatigue crack growth [10], it is expected that 17 mHz sinewave results should fall in the higher category and 60 sec ramp/reset results should reside in the low growth rate category. The fact that some exceptions do exist may be due to material variability, or to the somewhat delicate balance among the waveform, material, and the hydrogen assistance and oxide filming mechanisms which pertain to this type of testing.

Table 2 - Main Test Matrix (Unirradiated Materials)

	R = 0.2		R = 0.5		R = 0.7	
	1 cpm Sinewave	1 min Ramp	1 cpm Sinewave	1 min Ramp	1 cpm Sinewave	1 min Ramp
A508	4C+U	2C+U	D	D	1C+U	S+U
A533-B	2C+U	C+S	D	D	2C+U	S+U
Submerged Arc Welds						
Linde 80-Weld	2C+S	2C	D	D	2C	C+S
Linde 80 - HAZ (In A508-2)	2C	C+S	D	D	C+S	C+S
Linde 0091-Weld	2U+C	C+S	D	D	S+C	S+U
Linde 0091 - HAZ (In A533 B-1)	C	2S	D	D	S+U	2S
Linde 124-Weld	2C	2C	D	D	2C	2C
Linde 124 - HAZ (In A533 B-1)		C	D	D	U	C

Entries reflect combined Westinghouse and NRL effort.

S - Test scheduled
C - Test completed
D - Test deferred
U - Test underway

Table 3 - Tests in Progress - 31 March 1980 - NRL

Test Stand	Material	Conditions
1T Autoclave	A533-B-Round Robin	1 Hz sinewave R = 0.2
2/4T Autoclave	Irradiated A508-2	17 mHz sinewave R = 0.2
Multispecimen No. 1	A533-B A508-2 A516 Mn-Mo Weld (Linde 0091 Flux)	60 sec. ramp 1 sec. reset R = 0.2
Multispecimen No. 2	A106-C A508-2 A533B Mn-Mo Weld (Linde 0091 Flux)	60 sec. ramp 1 sec. reset R = 0.7
Multispecimen No. 3	A508-2 (3 Specs.) (Test just completed)	1800 sec. ramp 180 sec. hold R = 0.1

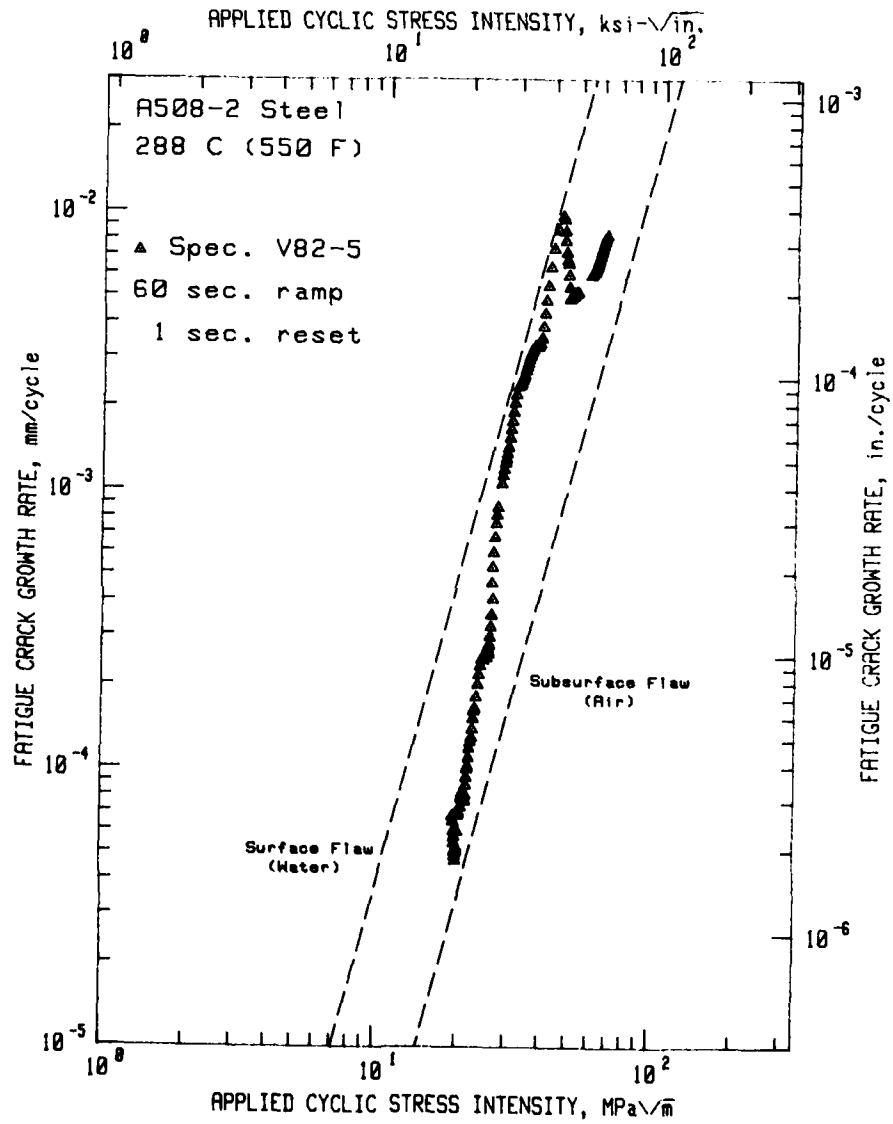

Fig. 8 — Fatigue crack growth rates vs applied cyclic stress intensity factor for A508-2 steel in the high-temperature, pressurized reactor-grade water environment — PWR conditions. This particular heat of A508 yielded significantly higher crack growth rates than others tested at the NRL.

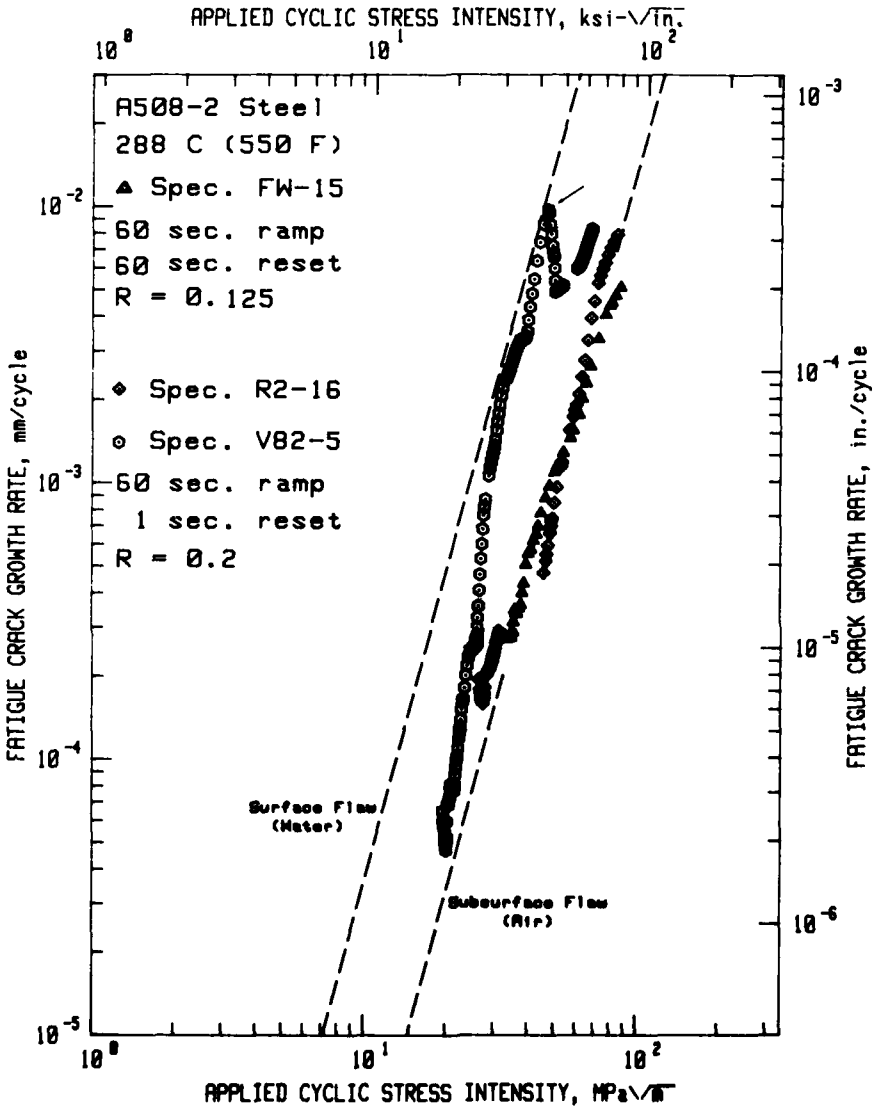

Fig. 9 — Fatigue crack growth rates vs applied cyclic stress intensity factors for A508-2 steel in the high-temperature, pressurized reactor-grade water environment — PWR conditions. This figure shows the rather high crack growth rates produced by the V82 heat as opposed to the FW and R heats. The peak in growth rates, denoted by the arrow, marks a point in the test at which a malfunctioning waveform generator applied an erratic signal to the system for about 30 hours of test time.

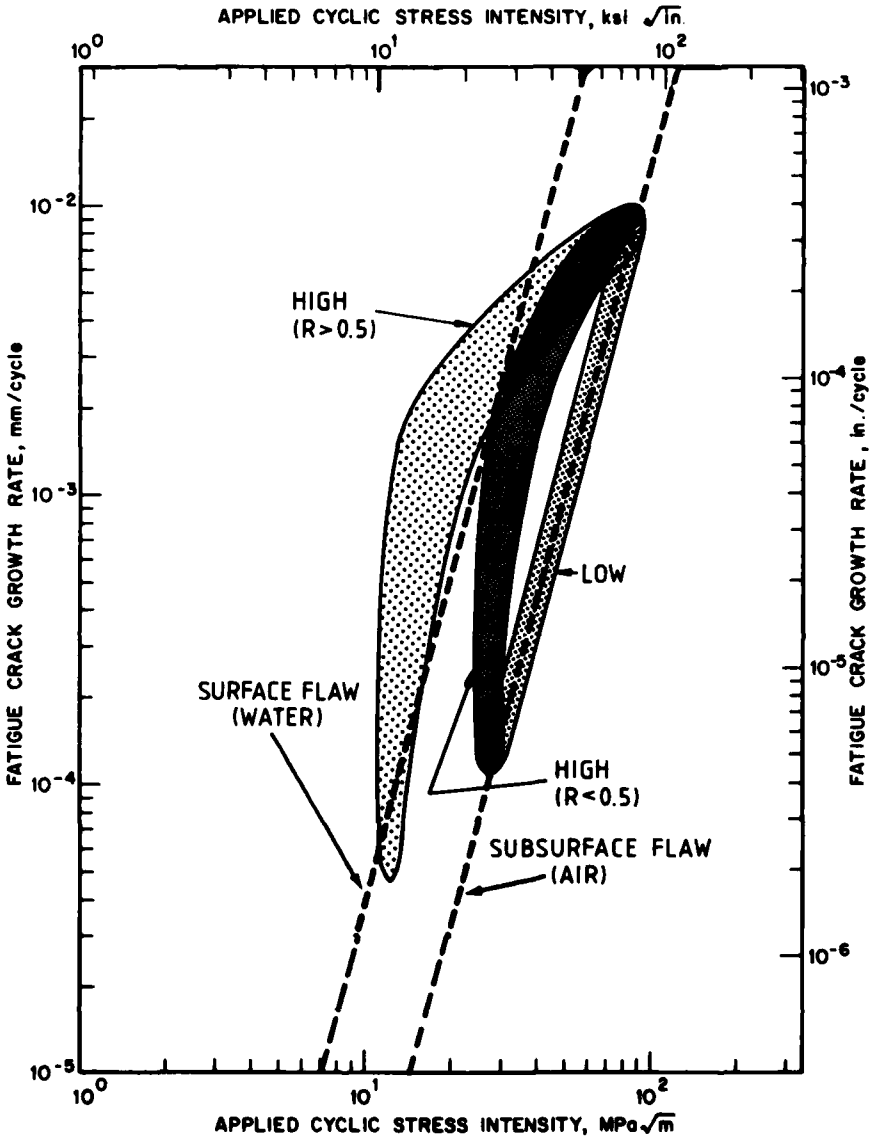

Fig. 10 — Summary of the trends in fatigue crack growth rates vs applied cyclic stress intensity factor for pressure vessel steels in high-temperature, pressurized reactor-grade water environment. As explained in the text, certain combinations of load ratio, waveform and frequency produce data residing in one of the shaded regions.

For load ratios of 0.7, there is no such clear distinction between the 17 mHz sinewave and 60 sec ramp/reset data—both reside in the shaded area designated "HIGH ($R > 0.5$)". That band is a fair representation of the trends of the R = 0.7 class of data, however, many of the individual data sets exhibit significant accelerations and decelerations which make their interpretation somewhat difficult.

An important element missing from the data acquired to date is an accurate determination of the values of fatigue crack growth rate at, or even near, the threshold value of the cyclic stress intensity factor. It is prohibitive to attempt to measure these rates for waveforms with periods of 60 seconds, since true threshold definition, involving measurements of growth rates in the 10^{-9} m/cycle (~4.0×10^{-8} in/cycle) range, or below requires a test of about 10^{8} cycles—equivalent to about 100 years of test time. But careful measurement of near-threshold growth rates, (of the order of 10^{-8} m/cycle (4×10^{-7} in./cycle), perhaps at higher cyclic frequencies, would serve to better define the expected behavior in this lower ΔK regime, an area which is nearly void of reliable data.

Of equal importance is the current lack of understanding of the relationships between steady-state fixed waveform fatigue crack growth rates and growth rates pertaining to the operating reactor situation, involving thermal cycling and variable amplitude loading. The planned NRL tests involving variable amplitude/variable frequency loading waveforms, and other tests at temperatures other than 288°C (550°F) will assist in identifying the seriousness of these potential problem areas.

b. Main Matrix Tests (Irradiated)

This facet of the main test matrix is being conducted at the NRL facilities. The status of main matrix tests of irradiated materials, both completed and underway, is shown in Table 4. The second test in this series was completed during this quarter. The results of this test, on irradiated A508-2 steel (Specimen Q71-9, 1T-CT) are shown in Fig. 11. Also shown, for comparison, are the results of an earlier test of this same material in an air environment at 288°C. These irradiated test results span a somewhat broader stress intensity factor range (~18 MPa$\sqrt{m}$ to 60 MPa$\sqrt{m}$) than did the first test, which was terminated well before any possibility of specimen failure. Figure 12, shows the results of the first irradiated test (specimen L83-6) described in the previous quarterly report, [12] together with results of tests at 288°C in an air environment. The environmental enhancement in the high-temperature, pressurized, reactor-grade water fatigue results has been very similar for both of these tests. However, as pointed out in the previous quarterly, the difference in results between irradiated and unirradiated steels, for the same reactor-grade water environment, are quite minimal, with the irradiated specimen results just slightly higher in crack growth rate.

During this quarter, a second autoclave, capable of testing 50 or 100 mm (2T or 4T) thick CT or WOL specimens, was installed in a hot cell and a test was started on 2T-CT specimen V82-1. This also is A508-2 steel, as was Q71-9, and the waveform (17 mHz sinewave) and stress intensity factor range (beginning at ~18 MPa$\sqrt{m}$) are also the same as in the smaller specimen test. This specimen (V82-1) was fatigued at 1 Hz in the 288°C, 14 MPa reactor-grade water environment over a range of ~15 to 18 MPa$\sqrt{m}$ to additionally extend the precrack before the actual test was begun.

Toward the end of this quarter, the 1T autoclave normally used for irradiated specimen testing was briefly devoted to a round-robin test for the International Cyclic Crack Growth Rate cooperative group, and then restored to the testing program for

Table 4 - Main Test Matrix (Irradiated Materials)

	R = 0.2		R = 0.5		R = 0.7	
	1 cpm Sinewave	1 min Ramp	1 cpm Sinewave	1 min Ramp	1 cpm Sinewave	1 min Ramp
A508	C+U	S	D	D	S	S
A533-B	C+S	S	D	D		2T
Submerged Arc Welds						
Linde 80-Weld	2T	2T	D	D	2T	2T
Linde 80 - HAZ (In A508-2)						
Linde 0091-Weld	2S	S	D	D	S+T	S+T
Linde 0091 - HAZ (In A533 B-1)						
Linde 124-Weld	2S					
Linde 124 - HAZ (In A533 B-1)						

Entries reflect combined Westinghouse and NRL effort.
Blank - No test or irradiation scheduled at present
C - Test completed
S - Test scheduled
T - Test tentative, pending other test results
D - Test deferred
U - Test underway

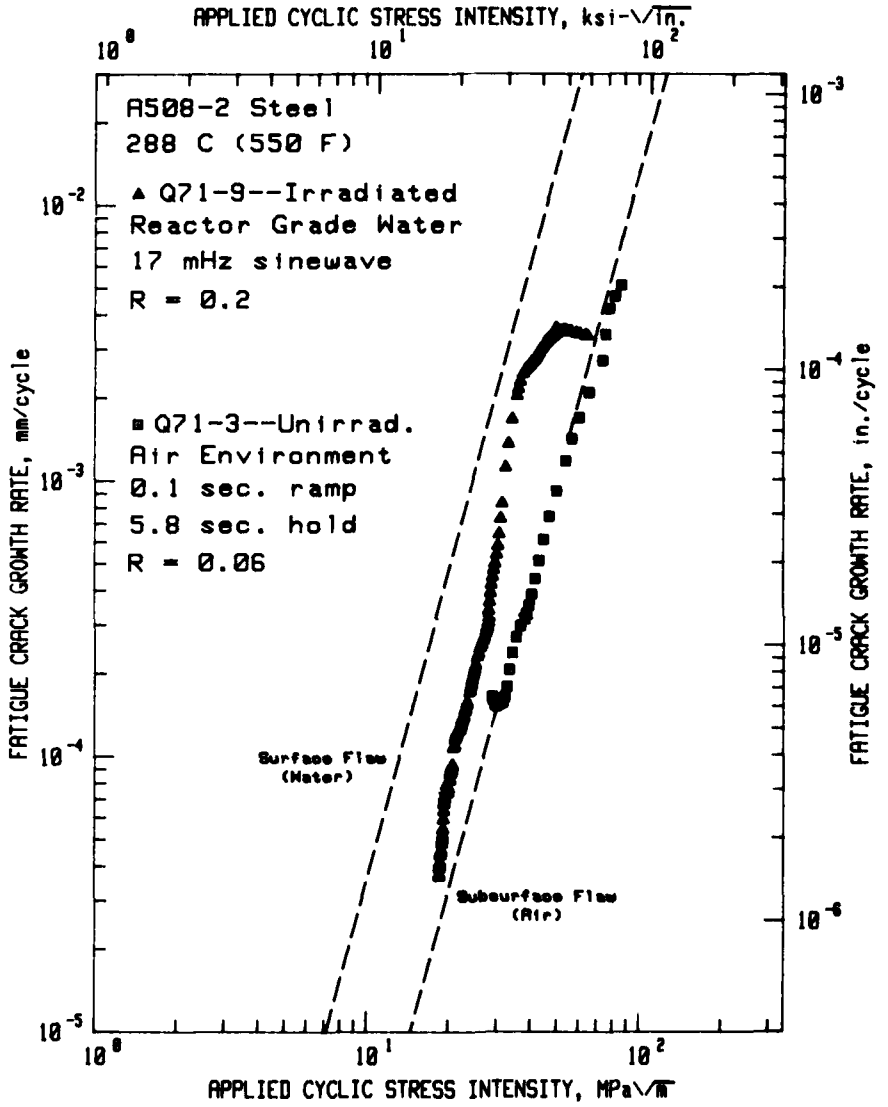

Fig. 11 — Fatigue crack growth rates vs applied cyclic stress intensity factors for irradiated A508-2 steel in the high-temperature, pressurized reactor-grade water—PWR conditions, and in a high-temperature air environment

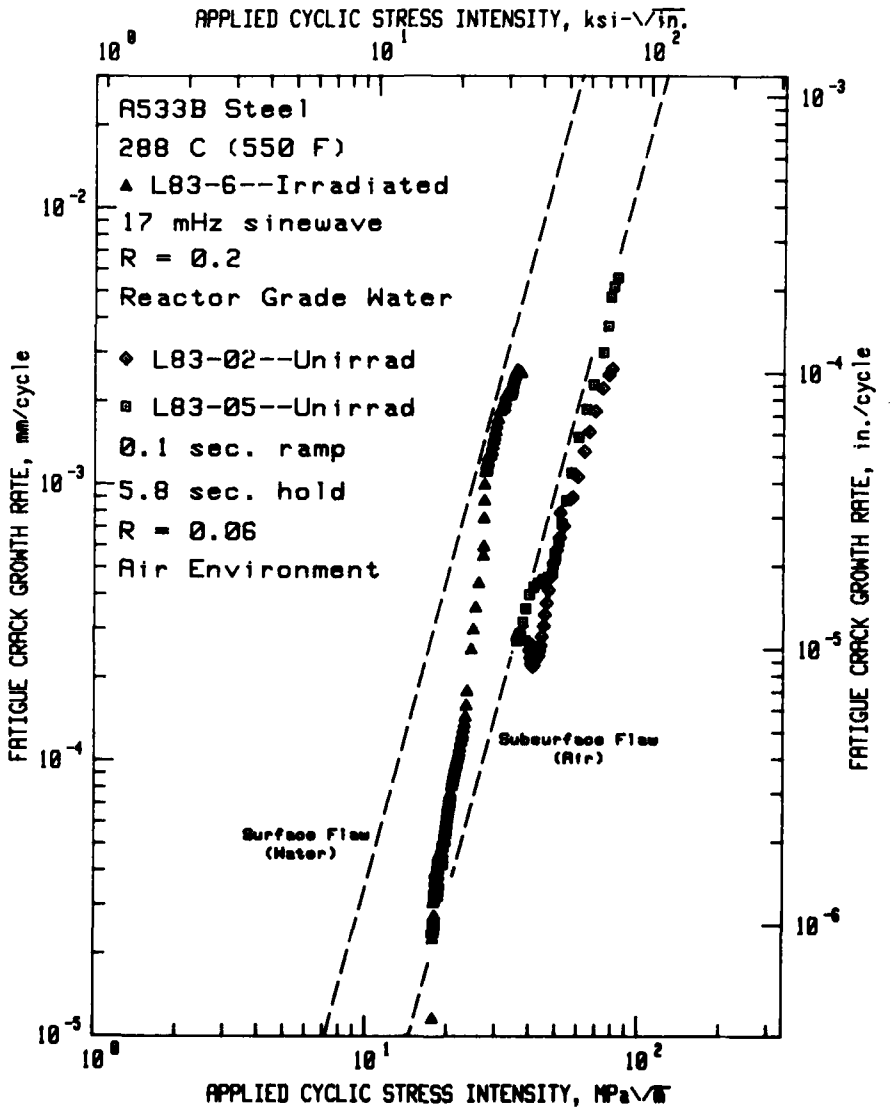

Fig. 12 — Fatigue crack growth rates vs applied cyclic stress intensity factors for irradiated A533-B steel in the high-temperature, pressurized reactor-grade water—PWR conditions, and in a high-temperature air environment

irradiated steels. The results of the round-robin test are detailed in the section on supporting tests.

c. Piping Test Matrix

As mentioned in the previous section, one specimen of A106-C steel (FOP-62), tested for about three months tested with a 60 sec ramp, 1 sec reset waveform, at a load ratio of 0.2 exhibited so little crack growth that the results cannot be meaningfully differentiated. This fact by itself is somewhat encouraging, implying that over a small ΔK range (~18 to 19 MPa$\sqrt{m}$), the material is quite immune to corrosion fatigue crack growth. Another specimen of A106-C remains under test at a load ratio, R, of 0.7, 60 sec ramp/1 sec reset waveform, and specimens of A106-C and A516 have just been started with a 17 mHz sinusoidal waveform and R = 0.2.

d. Variable Amplitude Tests

There is no data to report in this section for this quarter. Variable amplitude/variable frequency testing of four specimens of piping steels will begin in multispecimen autoclave #3 early in April, 1980. Fractographic results from the first variable amplitude test, on A516 steel are presented in the next section.

e. Supporting Tests

(1) Additional Fatigue Crack Growth Tests

As was clearly indicated in Ref. 10, a wide variety of waveforms involving various ramp times and hold times, and temperatures of 288°C, always produced corrosion fatigue crack growth rates in the low crack growth rate category, near the ASME Section XI air default line. The 17 mHz sinusoidal waveform tests have been the only consistent producers of fatigue data higher than this. In a continuing effort to determine the mechanistic basis underlying this phenomena, a series of tests involving ramp time/hold time approximations to 17 mHz sinusoidal waveforms have been carried out. Unfortunately, all the combinations attempted so far have failed to produce the high growth rates characteristic of sinusoidal waveforms. Two of these data sets, FW-15, (60 sec ramp, 60 sec reset) and R2-16 (60 sec ramp, 1 sec reset) were shown in Fig. 9. Two additional data sets, R2-14 (22 sec. ramp, 1 sec reset) and the most recently completed, R2-02 (22 sec ramp, 4 sec hold), are shown in Fig. 13. The test of R2-02 involved a piecewise linear approximation to a 17 mHz sinewave that differs only in the lack of "dwell" at the minimum load, and the decreasing ramp. In the classic interpretations of fatigue, neither of these are expected to contribute to fatigue crack growth. However, in view of these results, it is difficult to understand what characteristic of sinusoidal waveforms leads to such consistently higher growth rates.

While the 22 sec ramp/1 sec reset waveform produced low crack growth rate data at high temperature, a similar test, but at 93°C, resulted in some of the highest crack growth rates (for R=0.1 to 0.2) measured to date at the NRL. The results of this test are seen in Fig. 14. These results help to narrow the ramp time range over which low temperature FCGR results move from the low category to the high category. It is now clear that the conversion occurs between 1 sec (low) and 22 sec (high).

(2) ICCGR Round Robin Test #2

NRL is a participant in a round-robin test program conducted under the aegis of

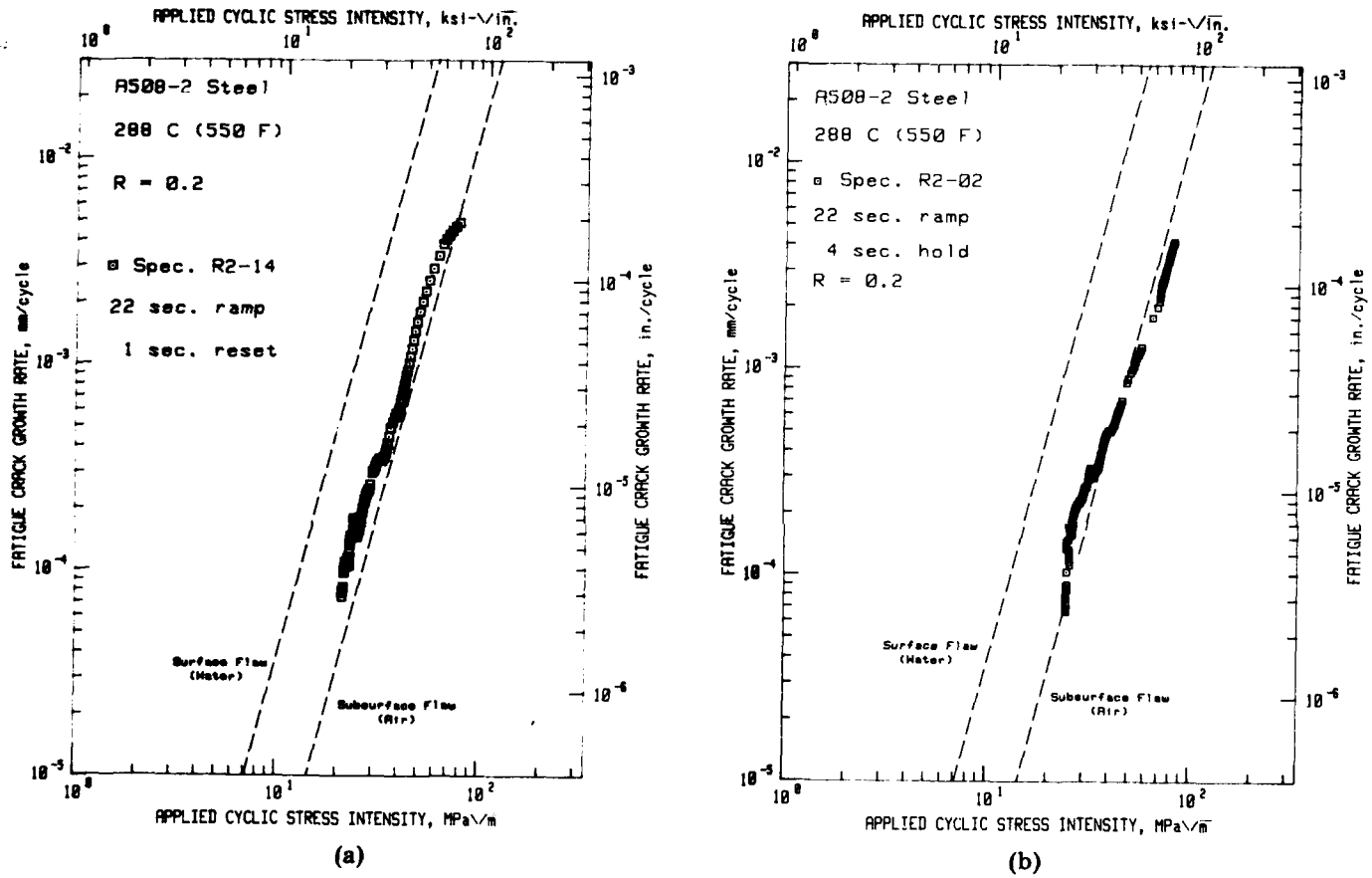

Fig. 13 — Fatigue crack growth rates vs applied cyclic stress intensity factors for two tests of A508-2 steel in the high-temperature, pressurized reactor-grade water—PWR conditions. Both of these tests represent attempts to model a 17 mHz sinusoidal waveform with ramp/hold waveform configuration. The sinewave results (Ref. 10) reside about midway between the ASME air and water default lines, bending over toward the air line at high ΔK values. Neither of these tests reproduce that behavior.

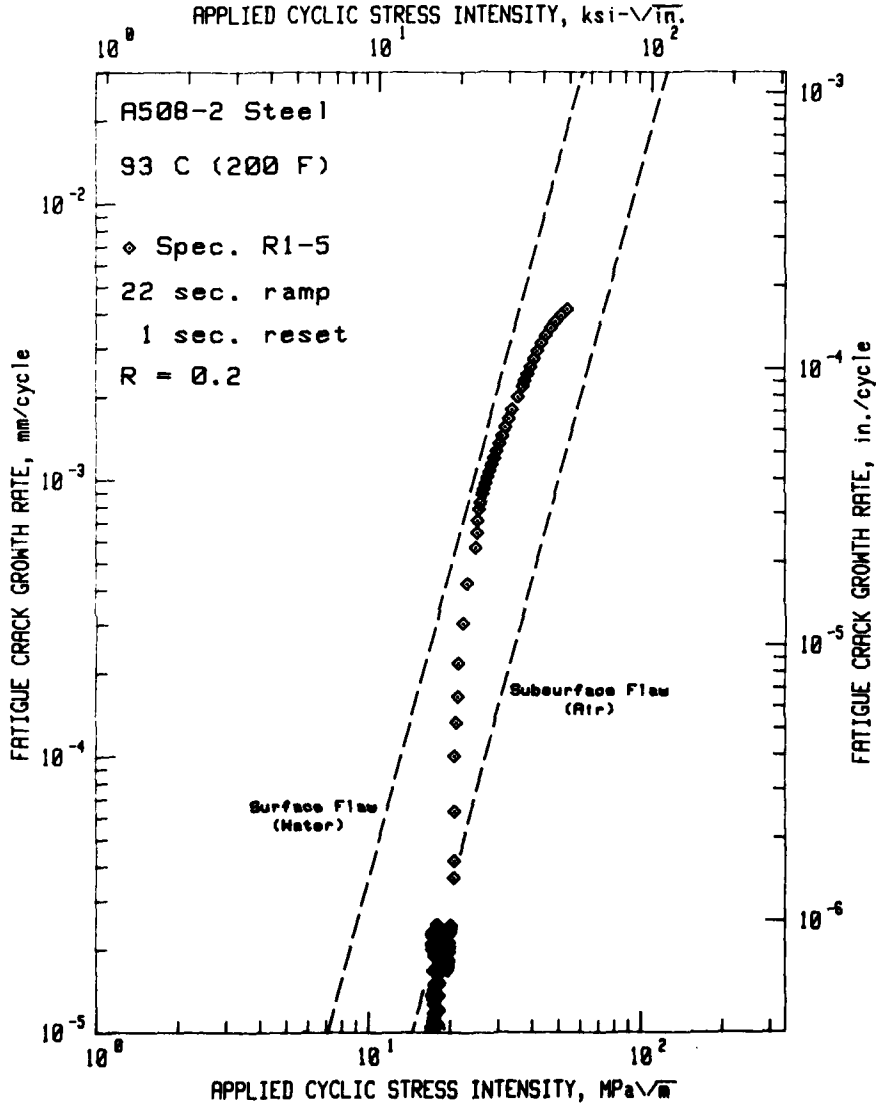

Fig. 14 — Fatigue crack growth rates vs applied cyclic stress intensity factors for A508-2 steel in a low-temperature, reactor-grade water environment—PWR conditions. Compared with Fig. 13a, the data shows a considerable environmentally assisted component. This data does fit the previously published model (Ref. 10) for fatigue crack growth in this environment.

the International Cyclic Crack Growth Rate cooperative group. About one year ago, the first test in the program, involving a 17 mHz sinusoidal waveform carried out at the NRL and at several other laboratories around the world. The NRL results from that test were originally reported in Ref. 1. When all the participating laboratories had reported their results, there was considerable variation in the measured crack growth rates. It has been suggested by NRL, and others, that variations in test practice, and variations in dissolved oxygen content of the aqueous environment could have produced large disparities in the results of these otherwise identical tests. As indicated in the previous item in this section (e-1- Additional Fatigue Crack Growth Tests) the 17 mHz sinusoidal waveform offers the greatest environmental susceptibility at 288°C, and it follows that variations in important environmental characteristics, such as dissolved oxygen content, would produce corresponding variations in the results.

With this basis in mind, the round-robin task leaders requested the participating laboratories to run a second test at the higher test frequency of 1 Hz, again with a sinusoidal waveform, and in the high-temperature, pressurized, deionized water environ ment. It is anticipated that the higher test frequency should minimize the environmentally assisted crack growth component, and the result in better agreement among the interlaboratory results. Figure 15 shows the NRL data from the first and second round-robin tests, and the trends in the results are very much as expected. Conducting the test at 1 Hz does minimize the environmental component and the crack growth rates reside essentially on the ASME Section XI air default line.

(3) Fractographic Results.

During September 1979, a variable amplitude, variable frequency test was conducted using a specimen of A516-C piping steel. The test environment was high-temperature, pressurized reactor-grade water (288°C, 14 MPa). The test conditions, including a description of the waveform, are included in Ref. [1]. The initial maximum applied stress intensity factor, K_{max}, was 44 MPa$\sqrt{m}$ (40 ksi$\sqrt{in}$). When the test had been concluded, it was discovered that the fatigue crack in specimen had rather severely branched, as shown in Fig. 16. Since the specimen was machined in the LT orientation, it was suspected that the rather high stress intensity factors, coupled with this orientation, resulted in the crack branching.

Figure 17 shows an SEM photograph of a typical region of the fatigue fracture surface of this specimen. Several different fracture modes are visible in the figure, including significant amounts of striated cleavage, ductile cleavage and several transverse cracks. Other areas of the specimen showed some intergranular fracture. Because of the severe branching, neither the stress intensity factor not the crack growth rates can be computed for the areas shown in Fig. 17. Additional future tests on other specimens from this heat of material may assist in the explanation of these features.

(4) Progress in Data Presentation

The accelerations and decelerations which occur, particularly in the early stages (low ΔK, da/dN $< 10^{-4}$ mm/cycle) of fatigue crack growth have been a subject of concern and conjecture among research scientists (and sponsors) involved in corrosion fatigue crack growth rate measurement on primary boundary materials for light water reactors. In order to help identify the external influences which may produce such reversals, Westinghouse and NRL introduced, in 1979, an intensified effort to upgrade the record-keeping associated with the test practice. As part of the post-test analysis,

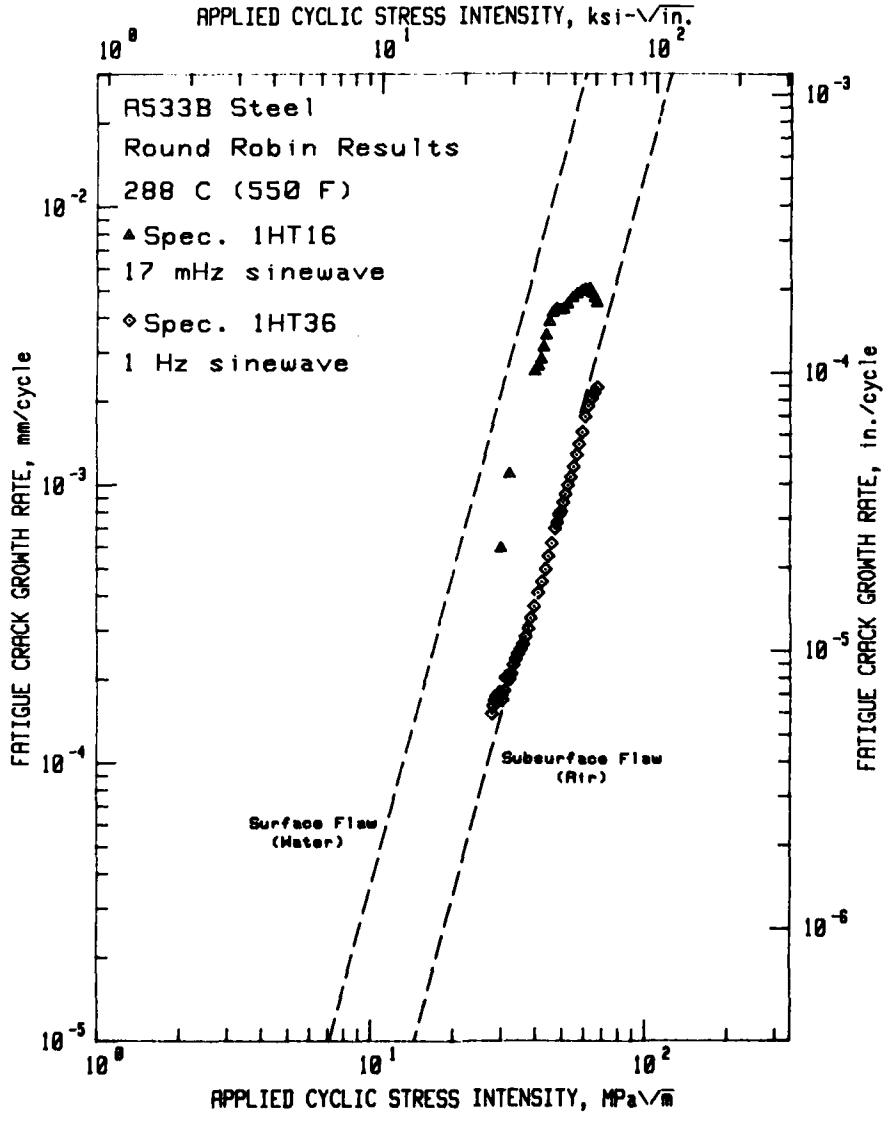

Fig. 15 — Fatigue crack growth rates vs applied cyclic stress intensity factors for two tests of A533B steel in high-temperature, pressurized reactor-grade water. These results are from the ICCGR round robin test efforts. The test at a 1 Hz frequency (1 HT36) shows no environmental assistance.

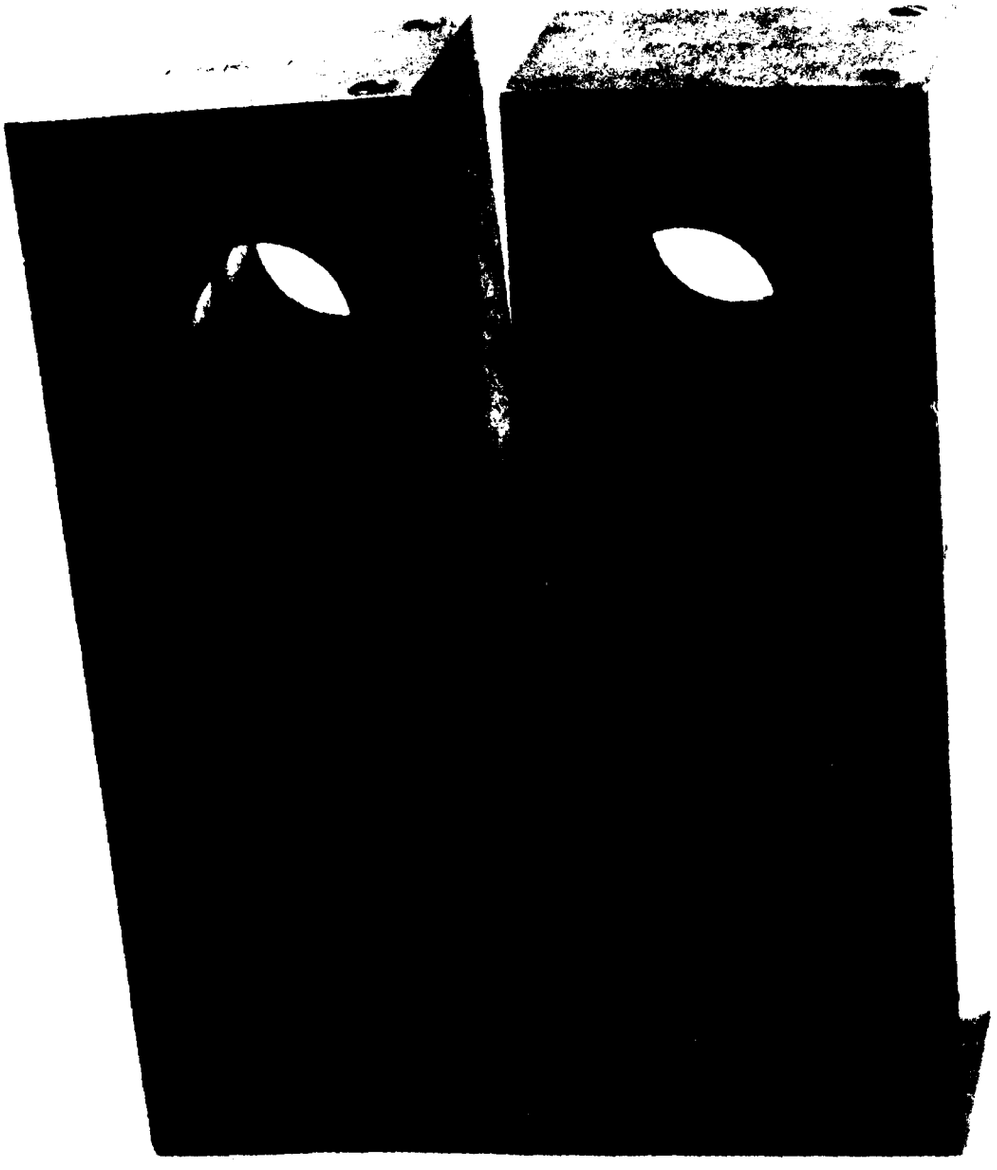

Fig. 16 — Photograph of specimen of A516-C piping steel used in variable amplitude, variable frequency fatigue crack growth test in the high-temperature, pressurized reactor-grade water environment. The extensive side-branching may be a product of the LT orientation of the crack with respect to the parent material.

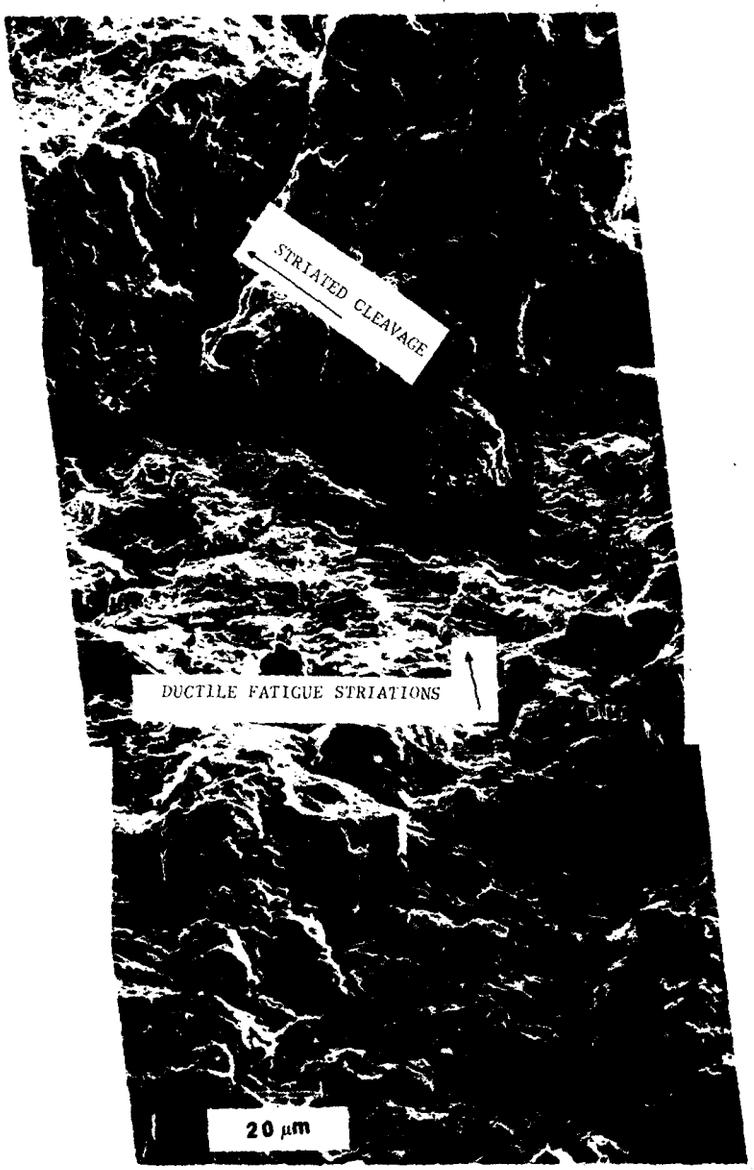

Fig. 17 — Scanning electron micrograph of the fatigue fracture surface of the specimen shown in Fig. 14. The overall crack propagation direction ran from bottom to top, as shown by the arrow. This section seems composed of a mixture of striated cleavage and ductile fatigue striation formation.

efforts have, and will, be made to associate interruptions or transients in the test procedures with the reversals or accelerations in the da/dN data.

To better facilitate the identification of these influences, a computer program to produce a da/dN vs N graph has been written. Figure 18 shows the results from three specimens in the same daisy chain. The absolute differences in fatigue crack growth rate are due to the three different initial values of ΔK appropriate to each specimen. The interesting feature is the lack of correlation of the variations between the specimen-to-specimen crack growth rates, and the general lack of correlation of growth rate transients to external influences, such as hydraulic or total system outages. Since the plot presents results from specimens tested in the same autoclave, at the same time, and therefore subject to the same water chemistry and other test practices, the only variable remaining is the material-to-material difference among the specimens. While confirmation of this conclusion will come only after analysis of several such tests, it would appear that many of the transients seen in FCGR data to date may be attributed to the material itself, or material-environment interactions which are basically a function of material properties.

COMMENTS ON TEST PRACTICE AT WESTINGHOUSE AND NRL

This continued testing in the high-temperature presurized water environment affords the opportunities to improve testing techniques and equipment, leading to enhanced integrity of the data. Similarly, the differences in the test practices between the two laboratories may result in some variability in crack growth rate data which can be related to the laboratory practice. Utilizing the results of improved record keeping procedures, the individual test histories can then be compared to the FCGR data itself, as in Fig. 18, to explain perturbations in the data, or they can be compared on a lab-to-lab basis to examine the important differences in test practice.

Because of the acknowledged influence of dissolved oxygen (DO_2) content on FCGR's for these material-environment combinations, much of the technical discussion and systems improvement have centered on this topic. For each of the four test systems at the NRL, on-line dissolved oxygen monitors provide a continuous read-out of the DO_2 content of the feedwater supply. The NRL practice is to deoxygenate the water in the system, by bubbling either hydrogen or nitrogen gas through the water, until the DO_2 levels reach 5 ppb or less. At this point the tests may begin, and the dissolved oxygen levels allowed to decrease to less then 1 ppb either by continued bubbling or the natural tendency of the system to scavenge DO_2.

To qualify the performance of the on-line dissolved oxygen monitors, a recent experiment was conducted in which a separate circulation loop was constructed and attached to the analysis loop of the 2/4T autoclave. This separate circulation loop, which was made of transparent tubing, contained several ampoules containing a colorimetric reagent used for DO_2 analysis in the low ppb range. After the on-line DO_2 monitor indicated a DO_2 level of about 1 ppb, this separate loop was valved off and the ampoules broken. They showed no visible color change, indicating levels of 5 ppb DO_2 or less.

The Westinghouse practice has been to allow a test to commence at somewhat higher levels of dissolved oxygen and to allow tests to run continuously at DO_2 levels of about 10 ppb. Many (but far from all) of the Westinghouse test results are characterized by initially high crack growth rates, followed by a sometimes extensive deceleration, then revision to the more or less monotonic increase in growth rates with applied stress

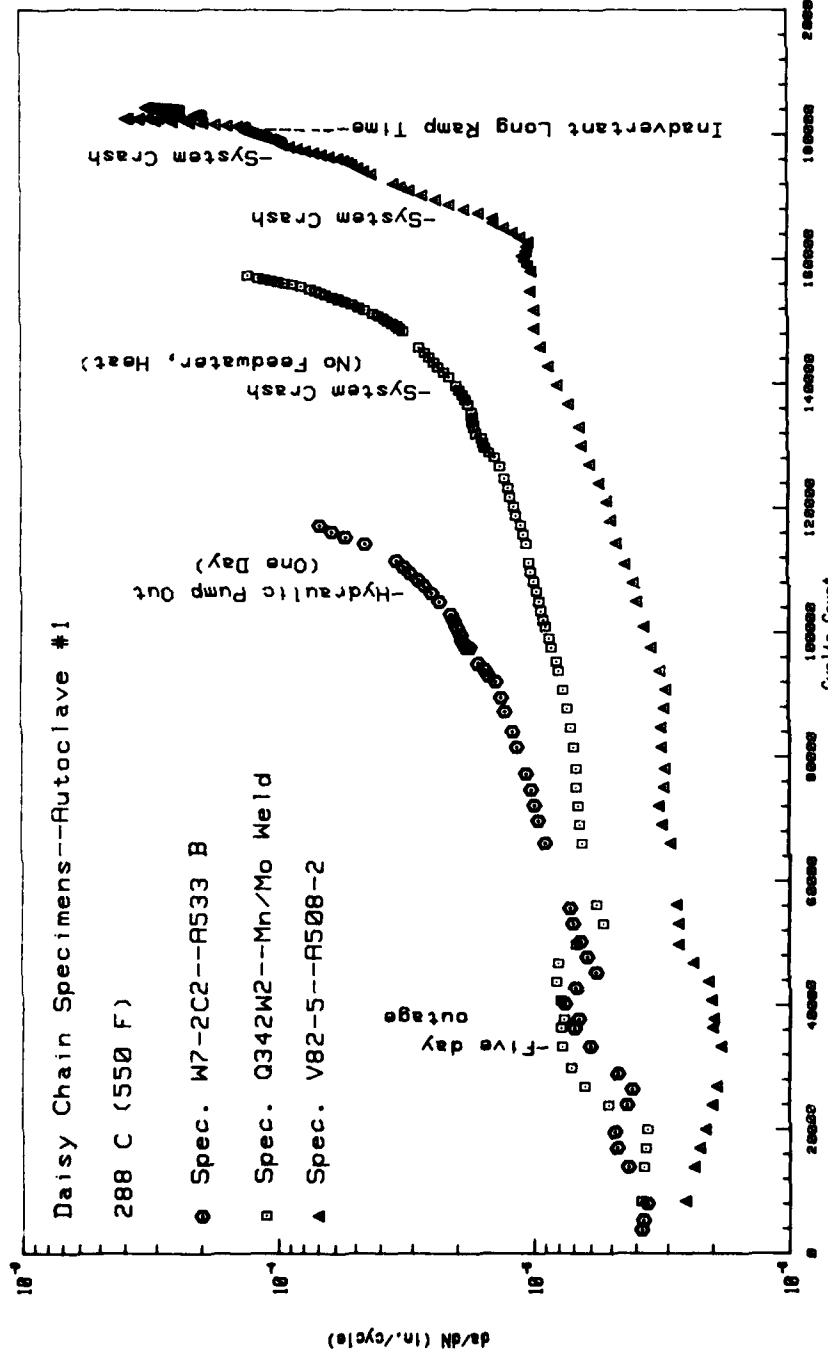

Fig. 18 — Fatigue crack growth rates vs total cyclic count for three specimens tested simultaneously in a multispecimen autoclave. This type of plot may be used to identify the influence (or lack of) of test practice on ensuing crack growth rates.

intensity. Although the idea is still in its speculative stages, it is possible that the initially high growth rates may be related to the initially high DO_2 levels. As the DO_2 levels decrease, so do the crack growth rates, at least to the point at which the mechanical driving energy outpaces the dissolved oxygen assistance to the FCGR's.

Many of the specimens currently under test at the NRL have been started out at a somewhat lower ΔK value (~15.5 MPa$\sqrt{m}$ for R=0.2, ~10 MPa$\sqrt{m}$ for R=0.7) than has been the customary practice. While the far lower FCGR's resulting from this practice adds measureably to the total test time required for each specimen, we feel that the enhanced quality of the data will provide significantly better input on which to base any recommended changes to the ASME Section XI Code.

The Westinghouse practice of initiating tests by "fast-cycling", or propagating the crack over a small range of ΔK, at or below the test load levels, has now been adopted by the NRL. While this method is supposed to provide a smooth start-up characteristic, the initial results are somewhat mixed, with several specimens experiencing decelerations, some undergoing periods of constant da/dN (ΔK-independent) growth, and some increasing monotonically with ΔK. After several such tests, the results will be summarized in some future quarterly report.

On somewhat the same topic, the Westinghouse laboratories continue to publish data supporting the starting ΔK effect. At the NRL, we are not actively engaged in starting ΔK research, but some accumulated results, which do not support the starting ΔK effect, have been published [14]. Since that time, the test results for one daisy chain of A508-2 specimens (R2-09,-11,-12) have been published [10] which also do not support the effect. In fact, the specimen with the highest initial ΔK, (R2-12) exhibited the highest relative FCGR, contrary to the expectations of the starting ΔK proponent.

B. Corrosion Fatigue Crack Growth Behavior of Pressure Vessel Steels

W. H. Bamford* and L. J. Ceschini*

INTRODUCTION

The objective of this program is to characterize the fatigue crack growth rate properties of ferritic pressure vessel steels exposed to PWR primary coolant environments. Three environmental chambers are being used, and the tests presently underway are listed in Table 5. Two areas are being investigated: characterization of weld/heat affected zone materials and study of mechanisms and starting effects.

Table 5 - Tests Underway as of March 1, 1980

Specimen	Loading Form	R. Ratio
D-1-WLD	0.017 Hz Sine Wave	0.20
D-2-WLD	0.017 Hz Sine Wave	0.70
D-2-HAZ	0.017 Hz Sine Wave	0.70

During this report period four specimens were completed under these two areas of investigation, all on the weld and heat-affected zone materials. This report will detail the results obtained, as well as the status of static bolt-loaded K_{ISCC} test specimens which are being tested in the bottom of the chambers.

CRACK GROWTH BEHAVIOR OF WELDS AND HEAT-AFFECTED ZONES

Tests of four weld and heat-affected zone specimens were completed during the reporting period. Individual test specimen results are shown in Fig. 19 to 22. Three of the specimens for which results were obtained are from a submerged arc weld using a Linde 80 flux in A508 Cl 2 forging steel, and the fourth is from the heat-affected zone of a submerged arc weld using a Linde 0091 flux, in A533 B Class 1 plate. These specimens are part of a matrix to study a number of different welds and heat-affected zones for nuclear grade pressure vessels, and the present status of the matrix is shown in Table 6. Testing emphasis during the next report period will be on the Linde 0091 weld and heat-affected zones.

Figure 19 shows the first results obtained for a heat-affected zone specimen tested under sinusoidal loading form at high R ratio. The growth rate in the specimen began at a relatively high rate (6×10^{-4} mm/cycle), then decreased very quickly to about 1×10^{-5} mm/cycle. This behavior is not entirely unlike that found for the weld metal specimens, as shown for example for C-7 WLD in Fig. 20. In this case no reversal occurred initially, but thereafter behavior was similar.

Figure 23 provides a comparison of corrosion fatigue crack growth behavior of two different heat-affected zones (HAZ) from submerged arc welds, one in A533 B Cl 1 plate and the other in A508 Cl 2 forging material. Note that, at least at R ratio = 0.2 there is virtually no difference in the results for these two specimens. The behavior closely parallels the behavior obtained for base metal specimens tested with the same loading form and frequency in the lower applied stress intensity factor (ΔK) regime, but is considerably more flattened than the bounding base metal behavior at higher ΔK.

*Westinghouse Electric Corporation.

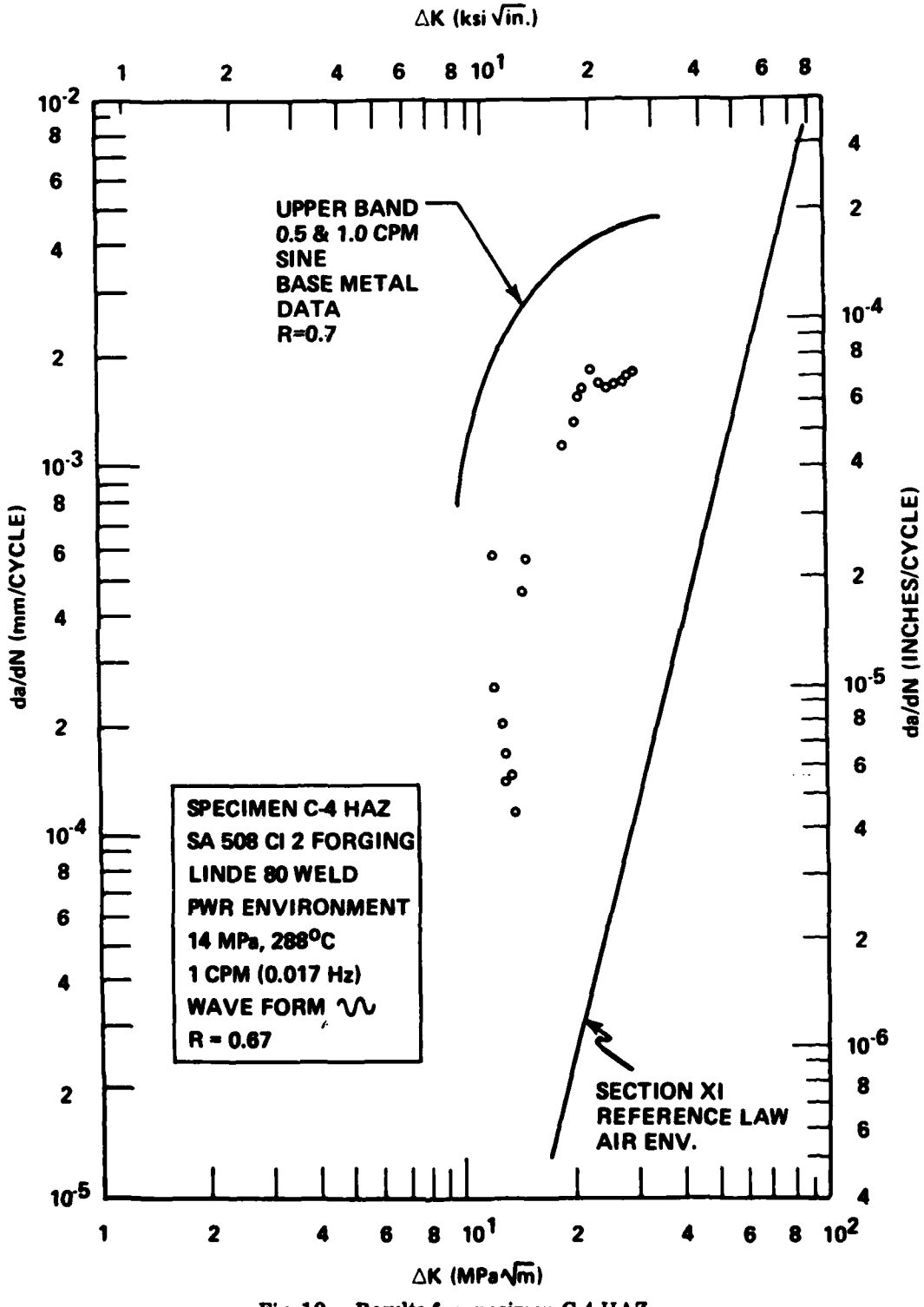

Fig. 19 — Results for specimen C-4-HAZ

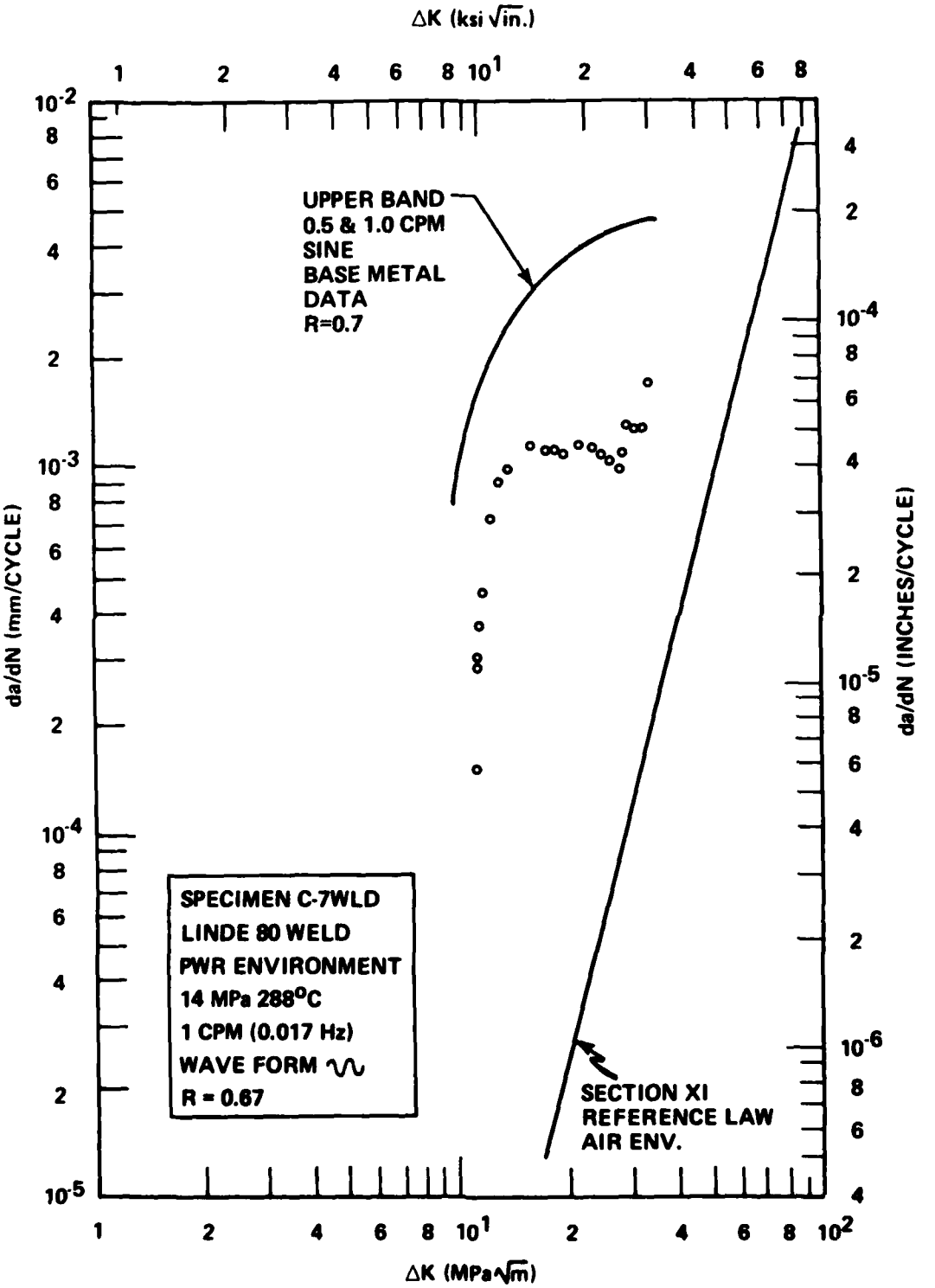

Fig. 20 — Results for specimen C-7-WLD

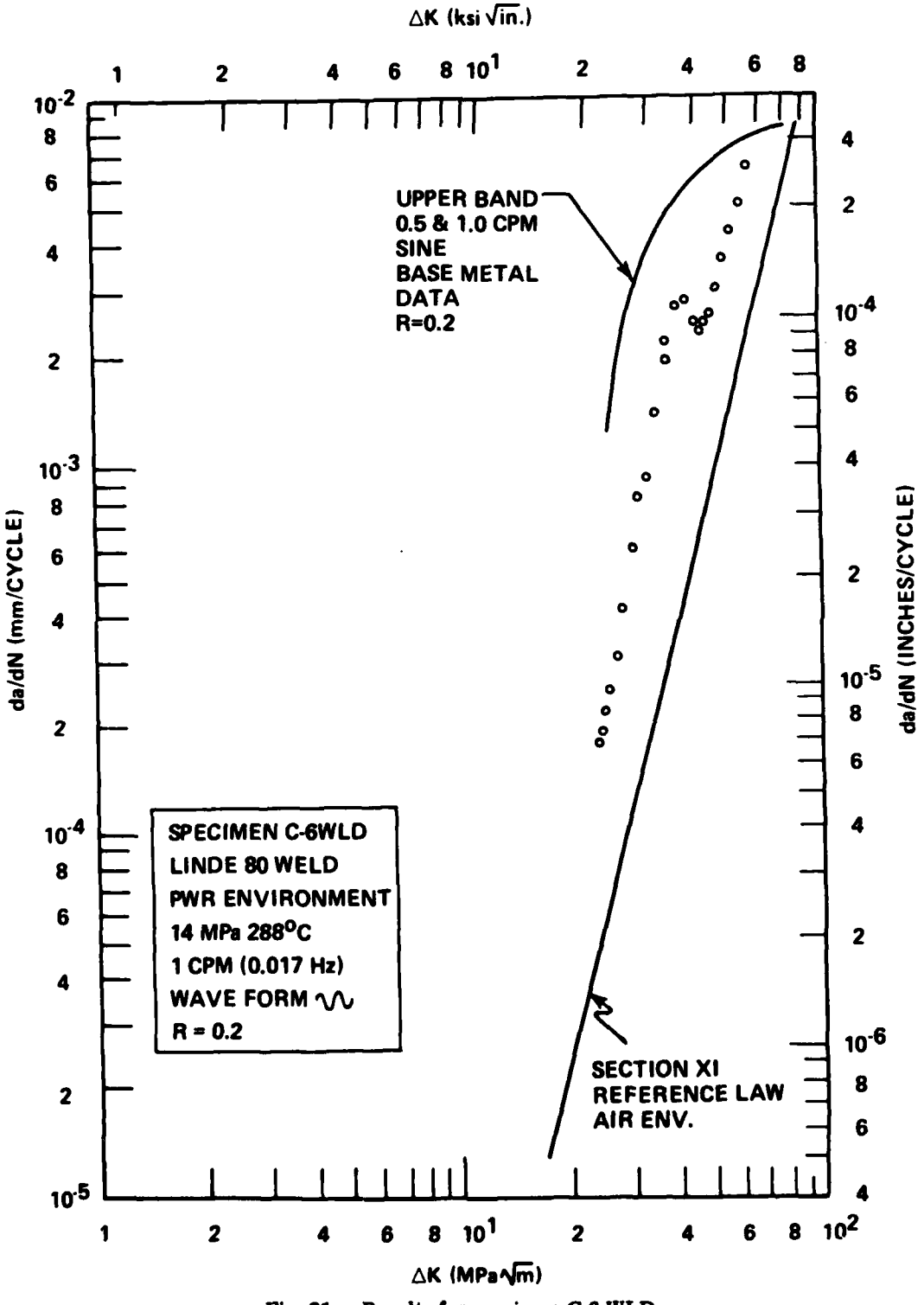

Fig. 21 — Results for specimen C-6-WLD

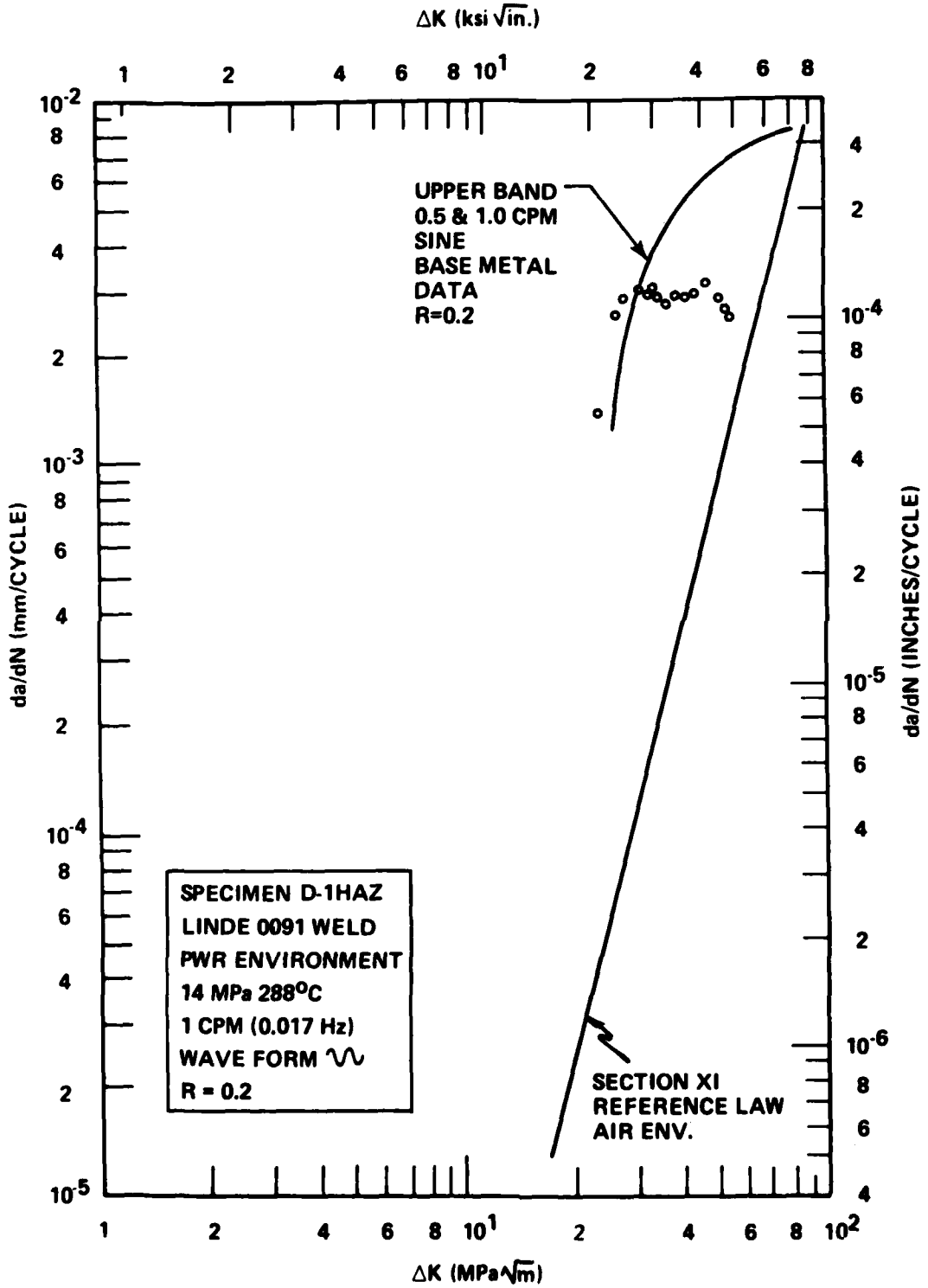

Fig. 22 — Results for specimen D-I-HAZ

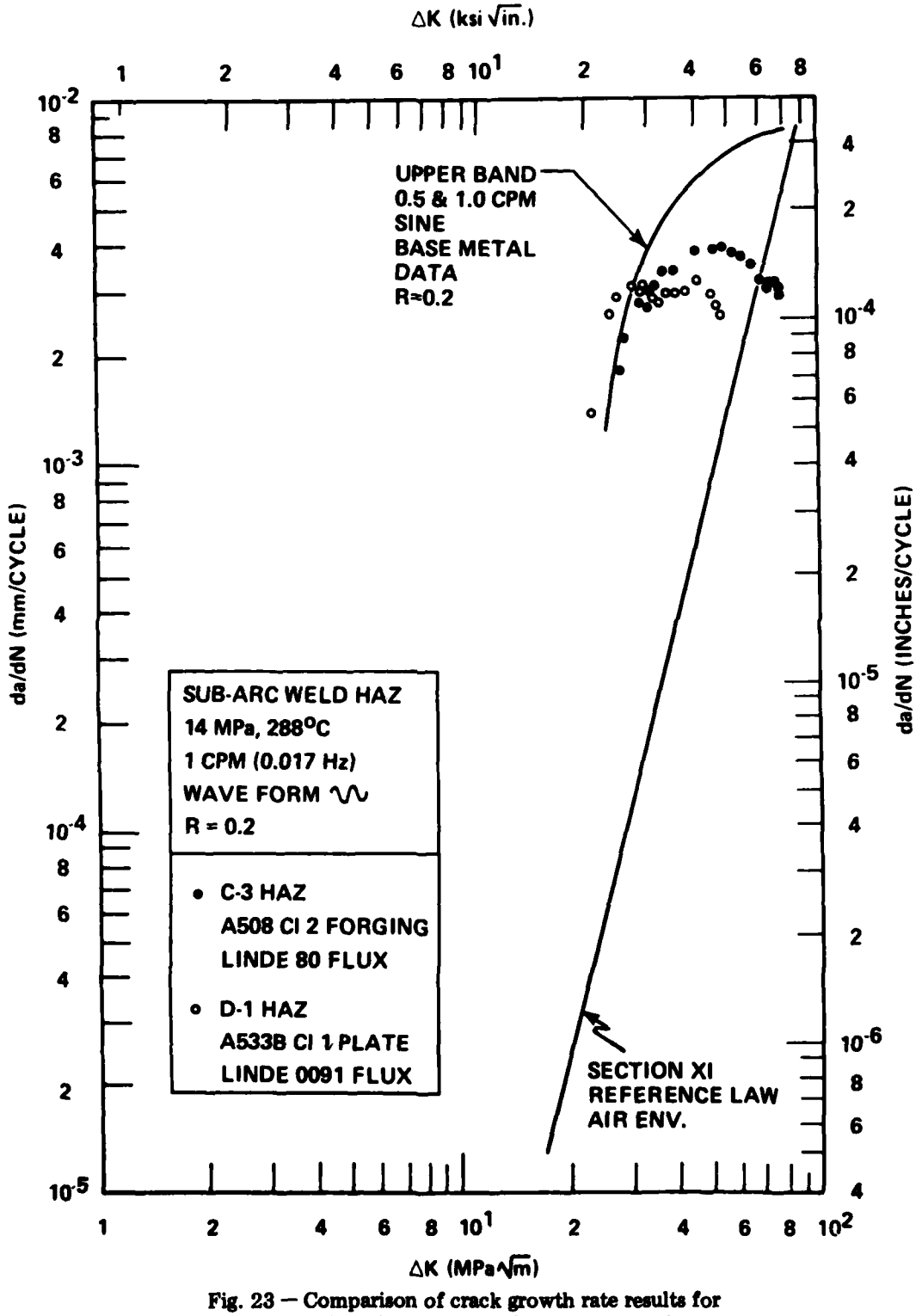

Fig. 23 — Comparison of crack growth rate results for heat-affected zone materials in ferritic steels

TABLE 6
Test Specimens Weld and Heat Affected Zones

Material	Test Conditions			
	R = 0.2		R = 0.7	
	One Cycle Per Minute	One Min-Ramp No Hold	One Cycle Per Minute	One Min-Ramp No Hold
Linde 124 Weld (2TWOL)	C-2 C-3	C-7 C-9	C-1 C-6	C-8 C-10
Linde 124 Weld HAZ (In A533B Cl 1 Plate) (2TCT)		C-24-HAZ-1		C-23-HAZ-1
Linde 80 Weld (2TCT)	C-3-WLD C-6-WLD*	C-1-WLD C-5-WLD	C-4-WLD C-7-WLD*	C-2-WLD
Linde 80 Weld HAZ (In A508 Cl 2 Forging) (2TCT)	C-3-HAZ	C-1-HAZ	C-4-HAZ*	C-2-HAZ
Linde 0091 Weld (2TCT)				
Linde 0091 Weld HAZ (In A533B cl 1 Plate) (2TCT)	D-1-HAZ*			

*Completed during this report period

This behavior will be further confirmed by future tests of heat-affected zone specimens from both steels, but is not unexpected. Results are not yet available for a similar comparison at high R ratio.

In Fig. 24, crack growth rate results are summarized for a submerged arc weld tested under the same loading wave form and R ratio as that used for the specimens in Fig. 23. In this case inconclusive results were obtained. Specimen C-3 WLD began to propagate at a fairly fast rate at the beginning of the test, similar to the HAZ specimens, but specimen C-6 WLD began to propagate at a much slower rate, almost an order of magnitude slower. The growth rate of specimen C-6 WLD increased with ΔK in a manner almost parallel with the air bahavior, while the growth rate of C-3 WLD did not increase significantly with ΔK. The behavior of the two specimens converged after ΔK became equal to about 36 MPa$\sqrt{m}$ (33 ksi$\sqrt{in}$), but then the growth rate of C-6 WLD began to increase again while C-3 began to approach the air growth rate behavior. The cause of this difference is presently unknown, but is being investigated.

The behavior of Linde 80 welds at high R ratio is summarized in Fig. 25, and shows that very similar results are obtained from the two specimens tested. The growth rate curve increases very quickly with ΔK until above 16 MPa$\sqrt{m}$ (14.5 ksi$\sqrt{in}$) and then flattens out considerably. This plateau occurs at a slightly higher growth rate for specimen C-4 WLD than for C-7 WLD, and is more of a pronounced plateau for C-7 WLD.

In all cases the growth rate behavior of these Linde 80 weld specimens has not exceeded the growth rates obtained for both plate and forging base metal specimens tested under similar conditions.

STATIC LOAD K_{Iscc} TESTING

The resistance of pressure vessel steels and typical welds and heat-affected zones to crack extension under static loading in the PWR environment has been under study in this program since 1974. The assessment is being carried out by means of bolt-loaded specimens which sit in the bottom of autoclaves being used for the fatigue crack growth rate testing. These specimens are removed for examination whenever the autoclave is taken down to replace a specimen or to perform a repair. Thus the specimens are subjected to PWR environment as well as air environment, similar to conditions which might exist for an operating reactor system.

There are presently 13 bolt-loaded specimens under test, including specimens from A533 B Cl-1, A508 Cl-2, a Linde 124 weld and two heat-affected zones. Some of these specimens have been loaded for as long as 42,200 hours, and none of the weld or base metal specimens have exhibited any crack extension. Crack extension has occurred in the heat-affected zone specimens, however, and to date every HAZ specimen under test has cracked further. After initiation in the HAZ cracks have extended into the weld and base metal. The status of all the specimens now under test is summarized Table 7.

The specimens have all been prepared in the same manner. They are precracked in air at low loadings in compliance with ASTM E 399 requirements, then loaded to a predetermined value of stress intensity factor, K, which is obtained by tightening the bolt until the face opening of the specimen corresponds to that K as determined by a compliance relationship [8]. If the crack propagates, it should stop at a length which corresponds to the threshold for stress corrosion cracking, K_{Iscc}. This value is easily calculated from the final crack length, because the face opening of the specimen

TABLE 7

STATUS OF BOLT-LOADED SPECIMENS IN SIMULATED PWR ENVIRONMENT

MARCH 1, 1980

Material	Specimen	Applied Stress Intensity Factor Ksi $\sqrt{in}$ (MPa $\sqrt{m}$)		Total Hours Loaded to Date	Hours in Environment
A533B Cl 1	04A-112	100	(110)	42205	34146
Plate	04A-114	90	(99)	42205	34146
(HSST Plate 4)	04A-116	80	(88)	42205	34146
A508 Cl 2	F-13	100	(110)	42812	35404
Forging	F-14	90	(99)	42812	35404
	F-15	80	(88)	42182	35404
Linde 124	C-13	100	(110)	42812	35404
Weld	C-14	90	(99)	42812	35404
Linde 80	C-9-HAZ	100	(110)	3700 (1396)*	2772 (1152)*
Weld	C-10-HAZ	90	(99)	3700 (1396)*	2772 (1396)*
HAZ	C-11-HAZ	80	(88)	3700 (1564)*	2772 (1308)*
	C-12-HAZ	70	(77)	3160 (1720)*	2704 (1504)*
Linde 124		90	(99)		
Weld HAZ	C-12-1-HAZ	90	(99)	3160 (1720)	2704 (1504)*

*Hours at first sign of cracking

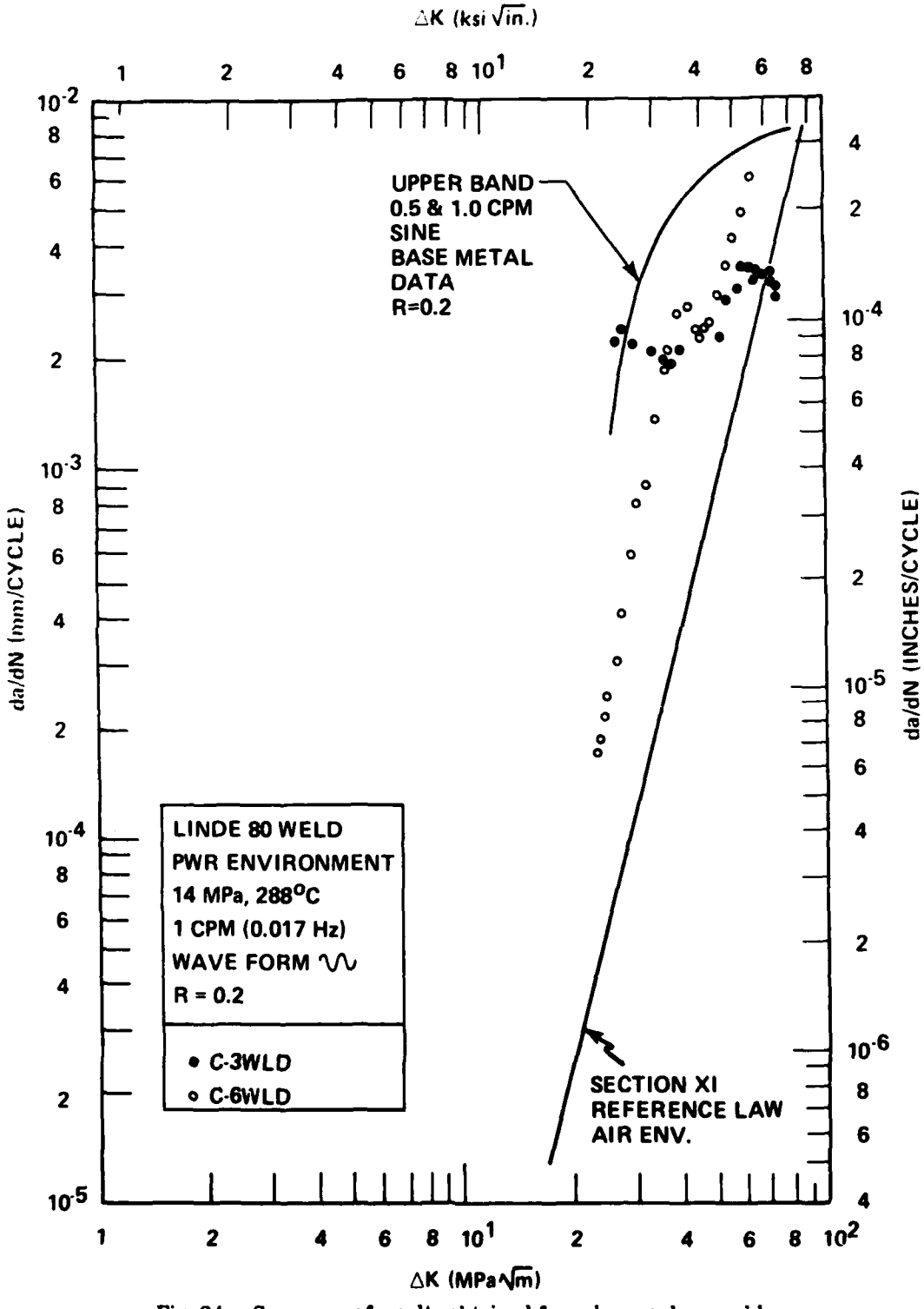

Fig. 24 — Summary of results obtained for submerged arc welds with Linde 80 flux, R = 0.2

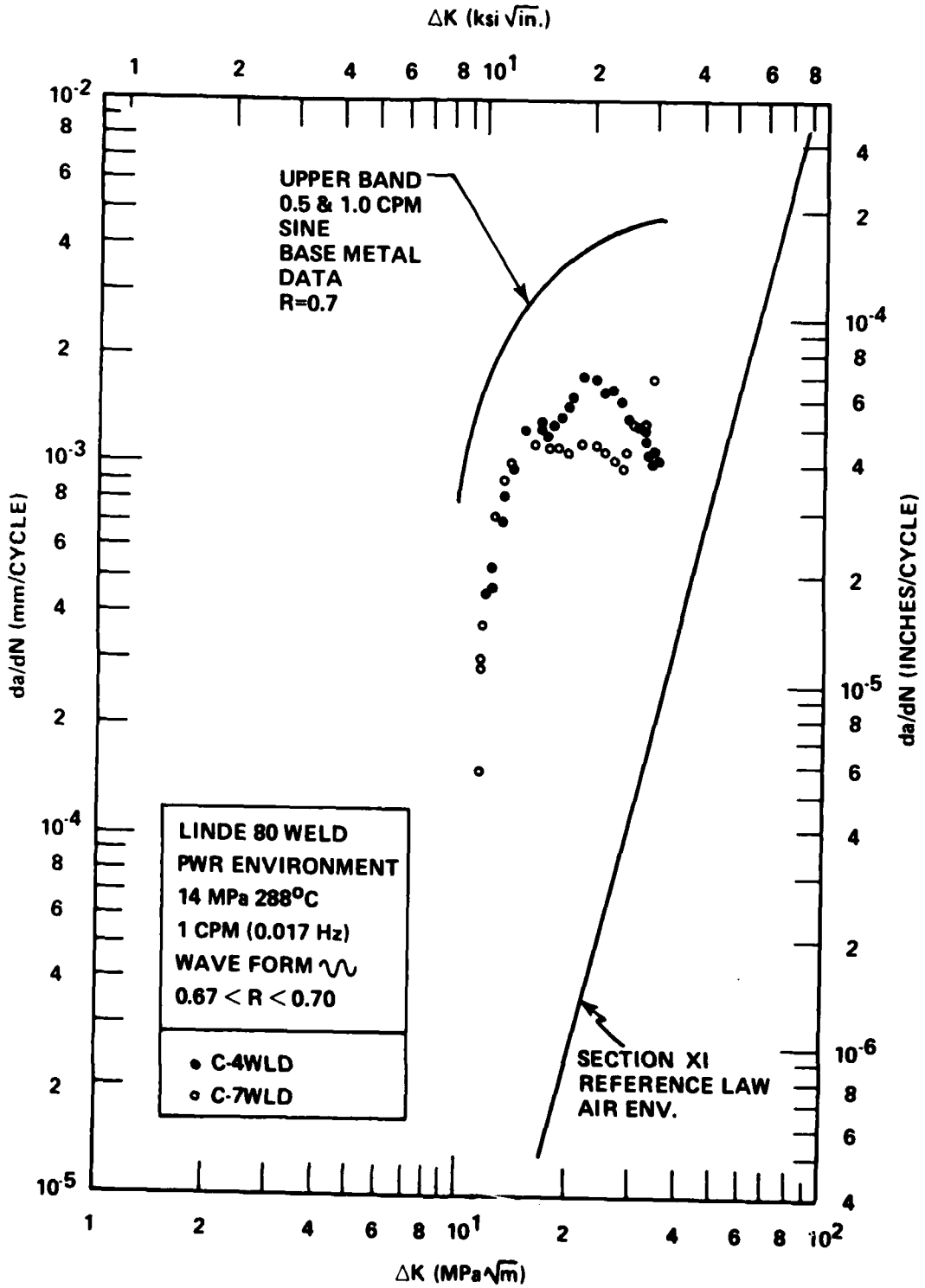

Fig. 25 — Summary of results obtained for submerged arc welds with Linde 80 flux, at high R ratio

remains constant even though the load drops as the crack propagates. Thus the applied K will decrease as the crack propagates, stopping at $K = K_{Iscc}$. This process is complicated considerably by the fact that incubation times are involved which may be very long in some cases. Even when cracking occurs, as it has in the HAZ specimens, it is irregular, and occurs by fits and starts. The method used to expose the specimens to the environment is somewhat deficient because the crack length can only be monitored periodically as the autoclave is opened for specimen insertion or repair of seals. Nonetheless, considerable information has been obtained on the behavior of these specimens through numerous removals. A history of the specimens which have shown cracking is presented in Table 8.

As can be seen in Table 8, crack extension appears to still be occurring in these specimens, with the tendency for cracks to propagate unevenly at first, and then for the cracks to even out on each side. As the cracks propagate into the specimen, the applied stress intensity factor K decreases, and should reach a common value for a given material regardless of the initial loading. This appeared to be occurring for the four HAZ specimens from the forging material, as seen in the next-to-last removal shown in Table 8; but at the last insertion it was found that two of the cracks had jumped to a very deep position, past a value of a/W = 0.85. Assessment of a value of K for a crack this deep is difficult and therefore unreliable, so values of K have not been provided pending further study of these two cases.

It is clear however that the value of K_{Iscc} for these HAZ materials can be much lower than previously thought, but it is not possible at this time to accurately define that value.

Crack extension was first observed in specimens C-9 and C-10 after 1152 hours of exposure, during the fall of 1979; and as a result two other specimens were added to the testing in the winter of 1979. These have now exhibited further cracking as well, and other specimens are planned for insertion in the near future.

The effect of weld heat input may be an important variable in the assessment of resistance to static load cracking; and this will be studied by both bolt-load and screening tests of several additional heat-affected zones, as well as welds.

TABLE 8

HISTORY OF BOLT LOADED SPECIMENS - HEAT-AFFECTED ZONE SPECIMENS

Specimen	Ksi $\sqrt{in.}$	($MP_a \sqrt{m}$)	Time in Environment Hours	Crack Length (Each Side) In. (cm)	Average Crack Length In. (cm)	Stress Intensity Factor Ksi $\sqrt{in.}$	($MP_a \sqrt{m}$)
C-9-HAZ	100	(110)	288	1.020/1.020 (2.59/2.59)	1.020 (2.59)	100.0	(110.0)
C-10-HAZ	90	(99)	288	1.020/1.020 (2.59/2.59)	1.020 (2.59)	90.0	(99.0)
C-11-HAZ	80	(88)	288	1.020/1.020 (2.59/2.59)	1.020 (2.59)	80.0	(88.0)
C-9-HAZ	100	(110)	1152	1.567/1.407 (3.98/3.57)	1.487 (3.78)	84.6	(93.1)
C-10-HAZ	90	(99)	1152	1.167/1.197 (2.96/3.04)	1.182 (3.00)	84.5	(92.9)
C-11-HAZ	80	(88)	1152	1.020/1.020 (2.59/2.59)	1.020 (2.59)	80.0	(88.0)
C-9-HAZ	100	(110)	1308	1.567/1.477 (3.98/3.75)	1.522 (3.87)	76.4	(84.0)
C-10-HAZ	90	(99)	1308	1.227/1.417 (3.12/3.60)	1.322 (3.36)	75.9	(83.6)
C-11-HAZ	80	(88)	1308	1.027/1.567 (2.61/3.98)	1.297 (3.29)	69.6	(76.6)
C-12-HAZ	70	(77)	356	1.020/1.020 (2.59/2.59)	1.020 (2.59)	70.0	(77.0)
C-12-1-HAZ	90	(99)	356	1.020/1.020 (2.59/2.59)	1.020 (2.59)	90.0	(99.0)
C-9-HAZ	100	(110)	1764	2.150/1.490 (5.46/3.78)	1.820 (4.63)	65.7	(72.3)
C-10-HAZ	90	(99)	1764	2.100/1.920 (5.33/4.88)	2.010 (5.11)	52.4	(57.6)
C-11-HAZ	80	(88)	1764	1.030/1.570 (2.62/3.99)	1.300 (3.30)	68.6	(75.5)
C-12-HAZ	70	(77)	452	1.020/1.020 (2.59/2.59)	1.020 (2.59)	70.0	(77.0)
C-12-1-HAZ	90	(99)	452	1.020/1.020 (2.59/2.59)	1.020 (2.59)	90.0	(99.0)
C-9-HAZ	100	(110)	2100	2.150/1.490 (5.46/3.78)	1.820 (4.63)	65.7	(72.3)
C-10-HAZ	90	(99)	2100	2.100/1.920 (5.33/4.88)	2.010 (5.11)	52.4	(57.6)
C-11-HAZ	80	(88)	2100	1.520/1.670 (3.86/4.24)	1.600 (4.05)	58.4	(64.2)
C-12-HAZ	70	(77)	1504	1.270/1.420 (3.23/3.61)	1.350 (3.42)	58.3	(64.1)
C-12-1-HAZ	90	(99)	1504	1.250/1.250 (3.18/3.18)	1.250 (3.18)	79.2	(87.1)
C-9-HAZ	100	(110)	2772	2.150/1.570 (5.46/3.99)	1.860 (4.72)	64.1	(70.5)
C-10-HAZ	90	(99)	2772	2.100/1.920 (5.33/4.88)	2.010 (5.11)	52.4	(57.6)
C-11-HAZ	80	(88)	2772	2.170/2.270 (5.51/5.77)	2.220 (5.64)	---	---
C-12-HAZ	70	(77)	2704	2.190/2.190 (5.56/5.56)	2.190 (5.56)	---	---
C-12-1-HAZ	90	(99)	2704	2.170/2.120 (5.51/5.38)	2.150 (5.45)	44.0	(48.4)

III. RADIATION SENSITIVITY AND POSTIRRADIATION RECOVERY

A. IAR Program Investigations of Charpy-V Notch Ductility and Tensile Property Trends With Cyclic Postirradiation Annealing and Reirradiation

J. R. Hawthorne, H. E. Watson, and F. J. Loss

BACKGROUND

The IAR Program is investigating the notch ductility and tensile properties behavior of submerged arc weld deposits with irradiation (I) followed by two full cycles of postirradiation annealing (A) and reirradiation (R). The intent of the program is to identify the merits and potential of the method for the control of radiation-induced embrittlement in reactor pressure vessels.

In a previous progress report [15], the background and objectives of the program were outlined. The planned experimental test matrix (Table 9) was also discussed together with a description of the materials selected for study. Based on the findings with Experiments 1 and 2, 399°C (750°F)-168 hr annealing conditions were selected for investigation in Experiments 3 and 4; that is, a 343°C (650°F)-168 hr anneal did not appear to be a practical method for the control of radiation embrittlement in reactor vessels because of the frequency of annealing which would be required. A 399°C anneal, on the other hand, showed definite promise for this application.

TABLE 9 - Radiation Experiment Plan
[288°C (550°F) Irradiation]

Experiment Series	Specimen	Designation	Objective
1	C_v	IA	Explore recovery by 343 and 399°C (650 and 750°F) annealing
2	C_v	IAR	Explore reirradiation response of all three materials
3	CT, C_v	I through IARAR	Determine IARAR performance of Weld 1
4	CT, C_v	I through IARAR	Determine IARAR performance of of Weld 2

PROGRESS

A report compiling C_v test results from all experiments has been developed and will be submitted to the 1980 ASTM Radiation Effects Symposium to be held in Savannah, Georgia in June 1980 [16].

Comparisons of results from Experiments 3 and 4 versus Experiments 1 and 2 in general indicated good internal consistency of the data from separate experiments. Thus, good experimental reproducibility was proven and confirmed that, with the scheme used, the notch ductility of the welds in the IAR condition was superior to that of the I condition and that comparable annealing recovery was effected by the second cycle versus first cycle anneals (see example, Fig. 26). Additionally, the data for the IARAR condition showed that a significant benefit can be obtained with multiple annealing and reirradiation procedures compared to irradiation without annealing. This is illustrated in Fig. 27 from the summary report. We note that the apparent rate of reembrittlement after annealing is higher than that for non-annealed material but that this characteristic does not overshadow the basic benefits.

The report also provides tensile test results obtained from specimens (blanks) included in the same irradiation assemblies. (The blanks were machined after irradiation on a tracer-equipped lathe modified for remote operation). Several observations were possible from the results; the most important of which was that the change in yield strength paralleled the change in C_v transition temperature. That is, the postirradiation yield strengths of the welds in the IARAR condition were lower than the postirradiation strengths in the I condition (Table 10). Less than full recovery in yield strength was produced by the 399°C annealing treatment.

TABLE 10 - Tensile Test Results for I and IARAR Conditions

Weld Code	Condition	Yield Strength (MPa)[a]	Tensile Strength (MPa)
V86	I	101	115
	IARAR	95	111
	(Unirradiated)	(74)	(93)
V84	I	106	120
	IARAR	95	112
	(Unirradiated)	(74)	(92)

[a]0.2 percent offset (5.74 mm gage diameter specimens).

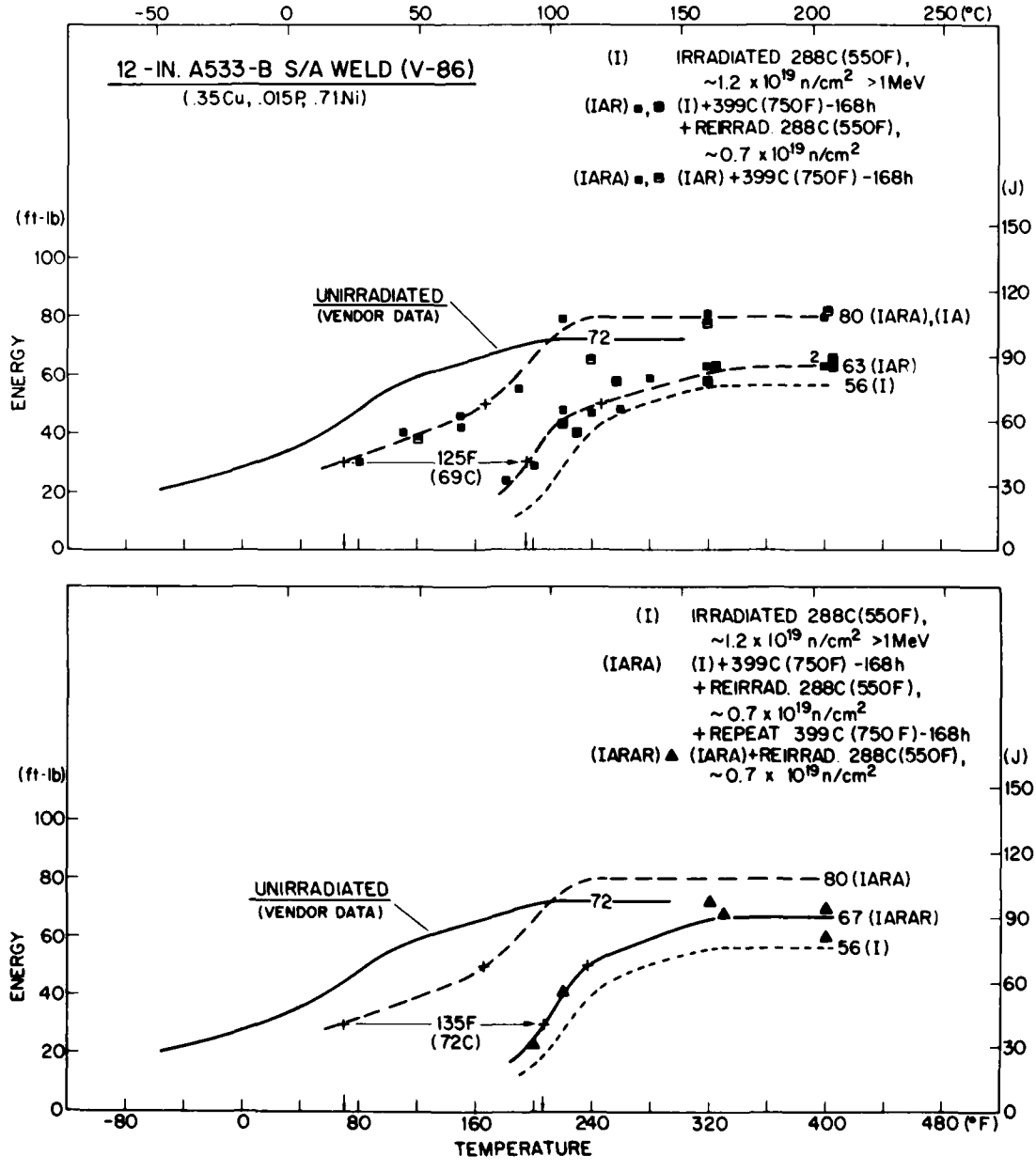

Fig. 26 — Charpy-V notch ductility of weld V86 in several conditions. The upper graph presents data for the irradiated (I) and reirradiated (IAR) conditions and for intermediate annealed (IA, IARA) conditions. The small symbols refer to prior Experiment 2 results; the larger symbols refer to Experiment 3 results. The lower graph presents data for the repeat reirradiation (IARAR) condition referenced to the trend curve for the first cycle irradiation (I) condition. A clear benefit of intermediate annealing is shown [16].

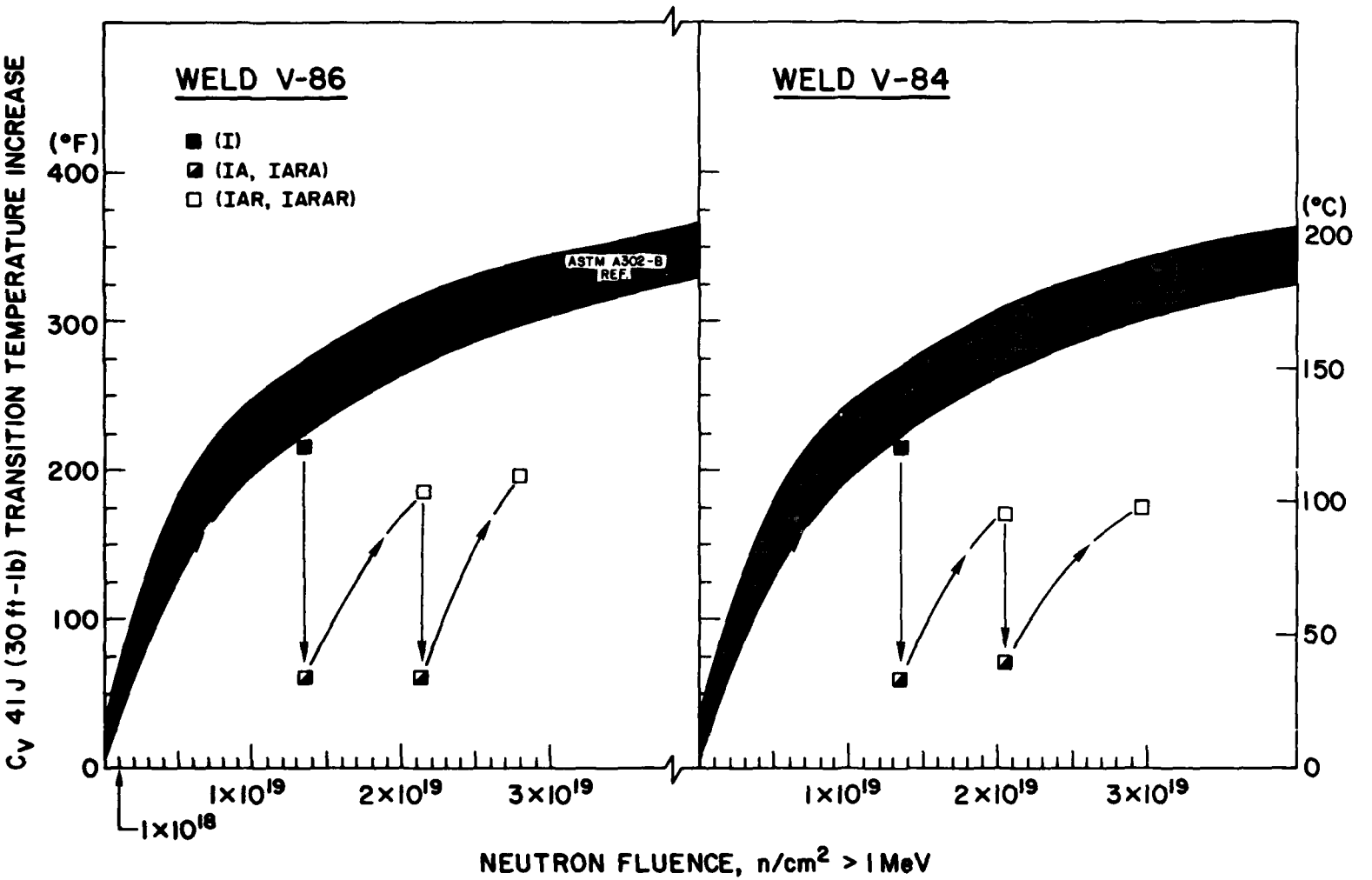

Fig. 27 — Transition temperature behavior of welds V86 and V84 with 288°C irradiation followed by two cycles of 399°C annealing and 288°C reirradiation. The shaded band refers to a data trend for the ASTM A302-B reference plate (0.21% Cu, 0.18% Ni), with <232°C irradiation; the lower boundary of this band appears to describe the 288°C embrittlement trend for the welds without intermediate annealing [16].

Essentially full recovery in tensile ductility was exhibited by the welds with annealing in parallel with their C_v upper shelf behavior. Further study of the relationship suggested by the two sets of data is in progress. It is proposed that ductility trends may prove quite important to attempts at correlating notch ductility and fracture toughness property trends where smooth and side grooved specimens, respectively, are being employed.

STATUS AND FINAL PLANS

Tests of compact toughness (CT) specimens included in Experiments 3 and 4 are largely completed; observations thus far are discussed in Ref. 17.

Phase 2 investigations have commenced with the procurement of additional weld metal stock comparable to the original welds (Codes V86 and V84). Phase 2 objectives include but are not limited to determinations of notch ductility trends as functions of first and second cycle fluence levels, re-embrittlement rates as a function of fluence, and time-temperature relationships in recovery. The Phase 2 studies will also extend the present investigation on the correlation of notch ductility and fracture toughness for irradiated, annealed and reirradiated conditions.

B. Evaluation and Comparison of IAEA Coordinated Program Steels and Welds With 288°C Irradiation

J. R. Hawthorne

BACKGROUND

The International Working Group on Reliability of Reactor Pressure Components (IWG-RRPC), sponsored by the International Atomic Energy Agency (IAEA), is conducting a coordinated study on the radiation embrittlement behavior of pressure vessel steels [18]. A primary goal of the program is to assess the radiation behavior of improved steels produced in various countries with the intent of demonstrating that a careful specification of reactor steels can eliminate the problem of potential failure including that caused by neutron irradiation and to demonstrate that knowledge has advanced to the point where steel manufacture and welding technology can routinely produce steel vessels of high radiation resistance [18].

The IWG-RRPC study encompasses plates, forgings and welds produced by the Federal Republic of Germany (FRG), France and Japan and a reference pressure vessel steel plate produced in the United States. The interests of NRL as a program participant include determination of the irradiation characteristics of overseas steel production, the relative radiation resistance of USA versus non-USA steel production, and the correlation of C_v notch ductility, fracture toughness, and strength changes produced by irradiation. Projected results will be of significant value to NRC Regulatory Guide 1.99 for foreign steel evaluations and to vessel construction codes since foreign steels have been employed extensively in some USA reactor vessels.

NRL radiation assessments of four materials supplied by Japan to the IWG-RRPC study have been reported [1]. The standard C_v and fatigue precracked C_v (PCC_v) specimens of these materials and the reference plate were irradiated in two reactor experiments at 288°C to about 1.5×10^{19} n/cm^2 >1 MeV. High radiation resistance was

generally observed. In addition, a possible correlation of transition temperature elevation measured by postirradiation C_v vs PCC_v tests was noted.

PROGRESS

During this reporting period, unirradiated condition C_v tests were completed for the remaining program materials supplied by France and the FRG. The experimental results are presented in Fig. 28 through 31 and are summarized in Table II. Note the relatively high brittle/ductile transition of the forging.

Additional progress relates to the completion of the reactor exposure of the French plate, weld and forging under temperature and fluence conditions matching those used for the Japanese materials. During this period, the construction of the irradiation unit for exposure of the FRG weld was also completed. Reactor insertion of this experiment is scheduled for late May.

FUTURE PLANS

Plans for the coming quarter include completion of unirradiated condition PCC_v tests of the remaining materials and completion of the reactor irradiation of the FRG weld deposit. Postirradiation tests of the French materials will also be initiated.

TABLE II - Charpy V-Notch Ductility of IWG-RRPC Program Materials Supplied by France and the FRG

Material	NRL Code	Transition Temperature (°C) 41 J	68 J	0.9 mm	Upper Shelf J
FRANCE					
Plate	FP	-18	7	-1	165
Forging	FF	~4	~35	27	200
Weld Deposit	FW	-54	-34	-40	193
FRG					
Weld Deposit	GW	-62	-51	-57	216

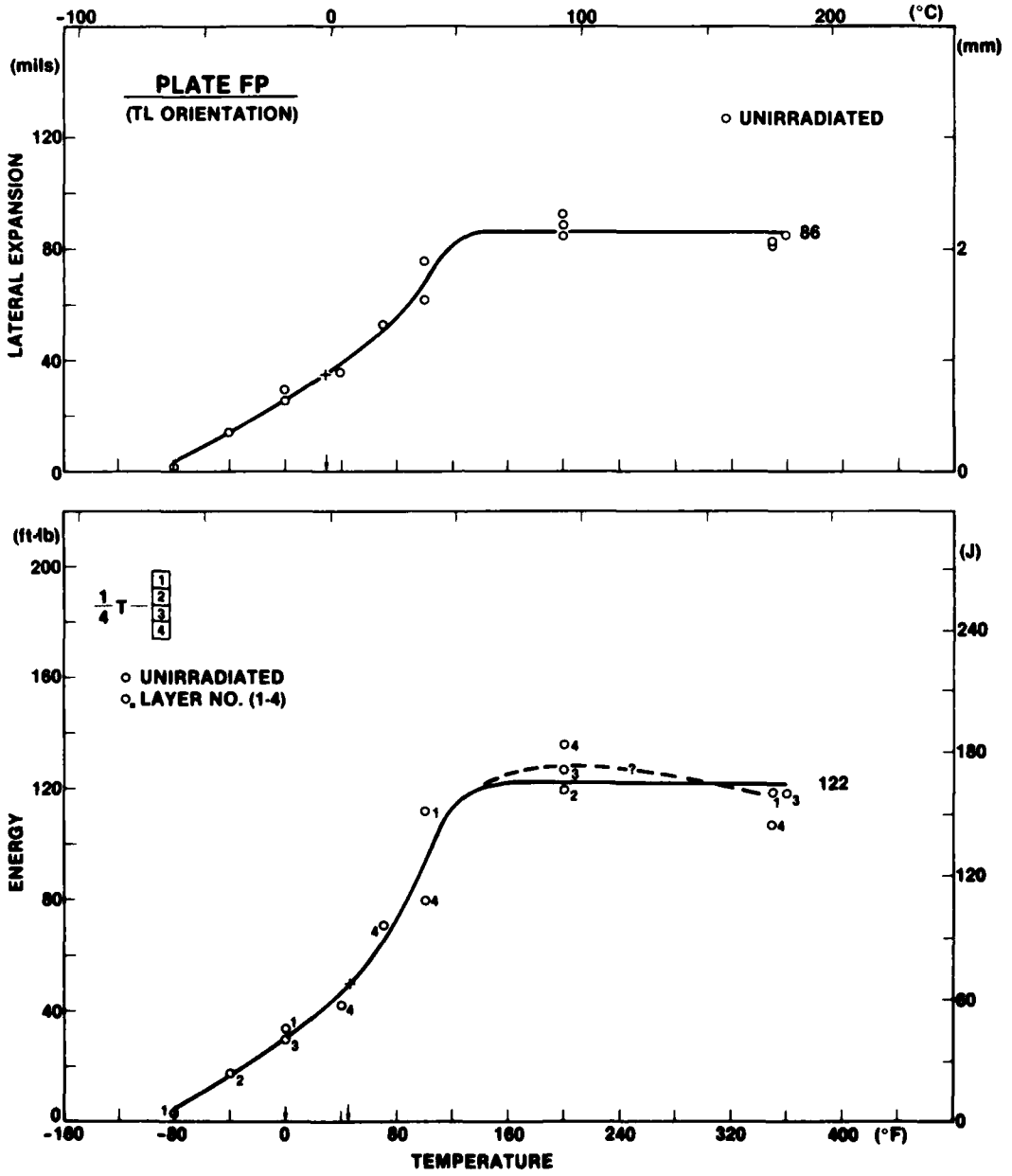

Fig. 28 — Charpy-V notch ductility of the A533-B Class 1 steel plate (Code FP) supplied by France to the IWG-RRPC cooperative program

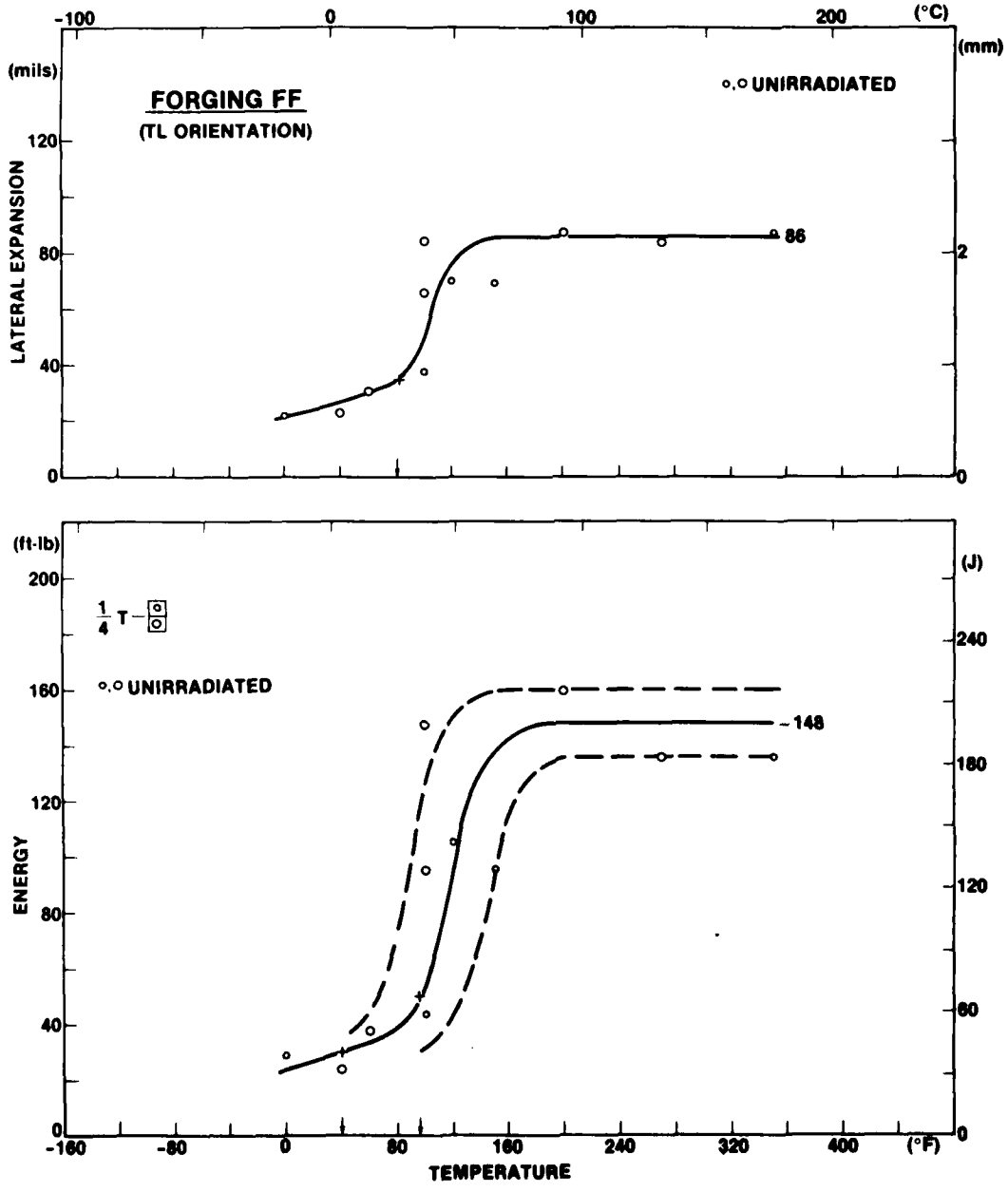

Fig. 29 — Charpy-V notch ductility of the A508 Class 3 steel forging (Code FF) supplied by France to the IWG-RRPC cooperative program

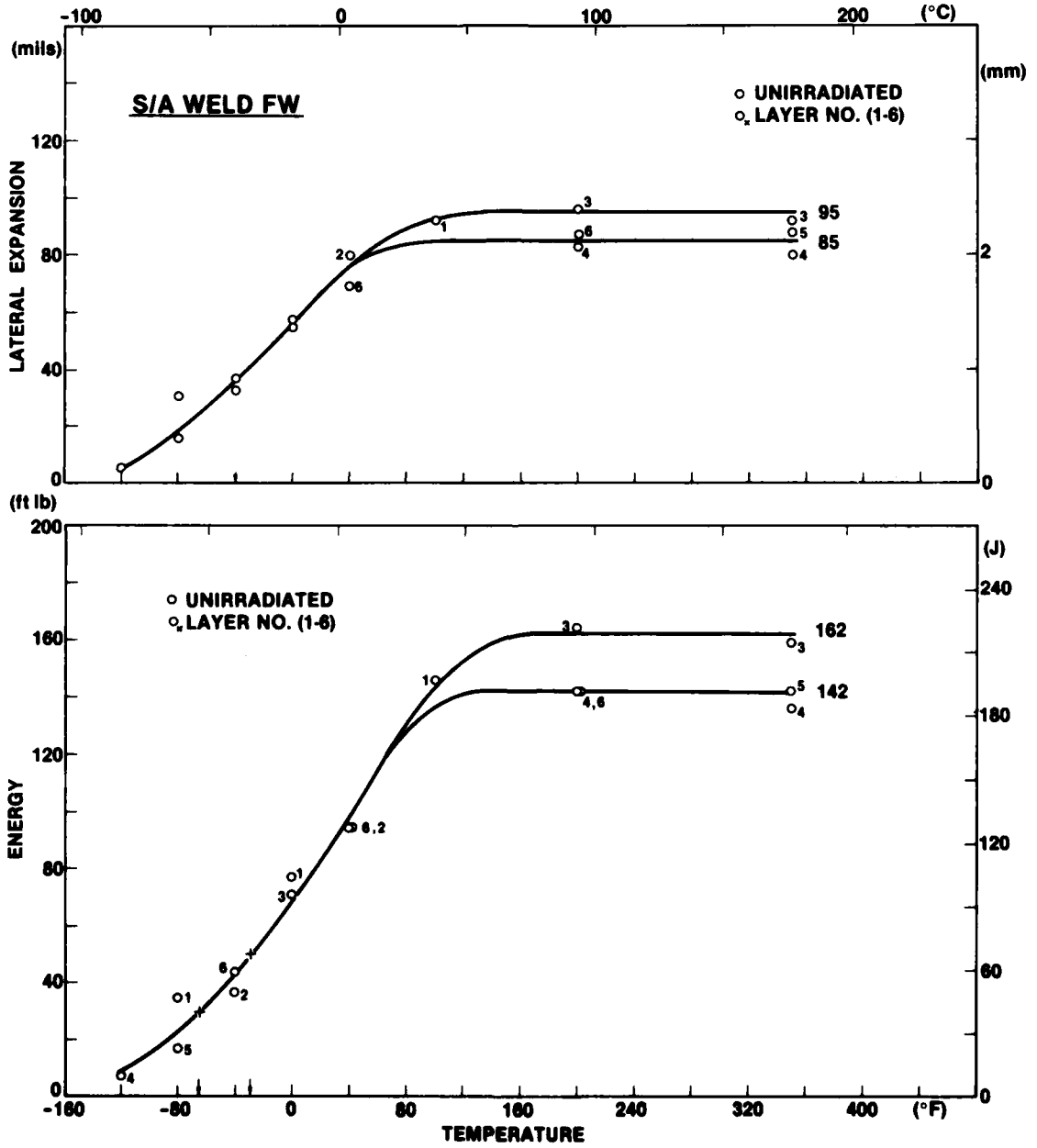

Fig. 30 — Charpy-V notch ductility of the submerged arc (S/A) weld (Code FW) supplied by France to the IWG-RRPC cooperative program

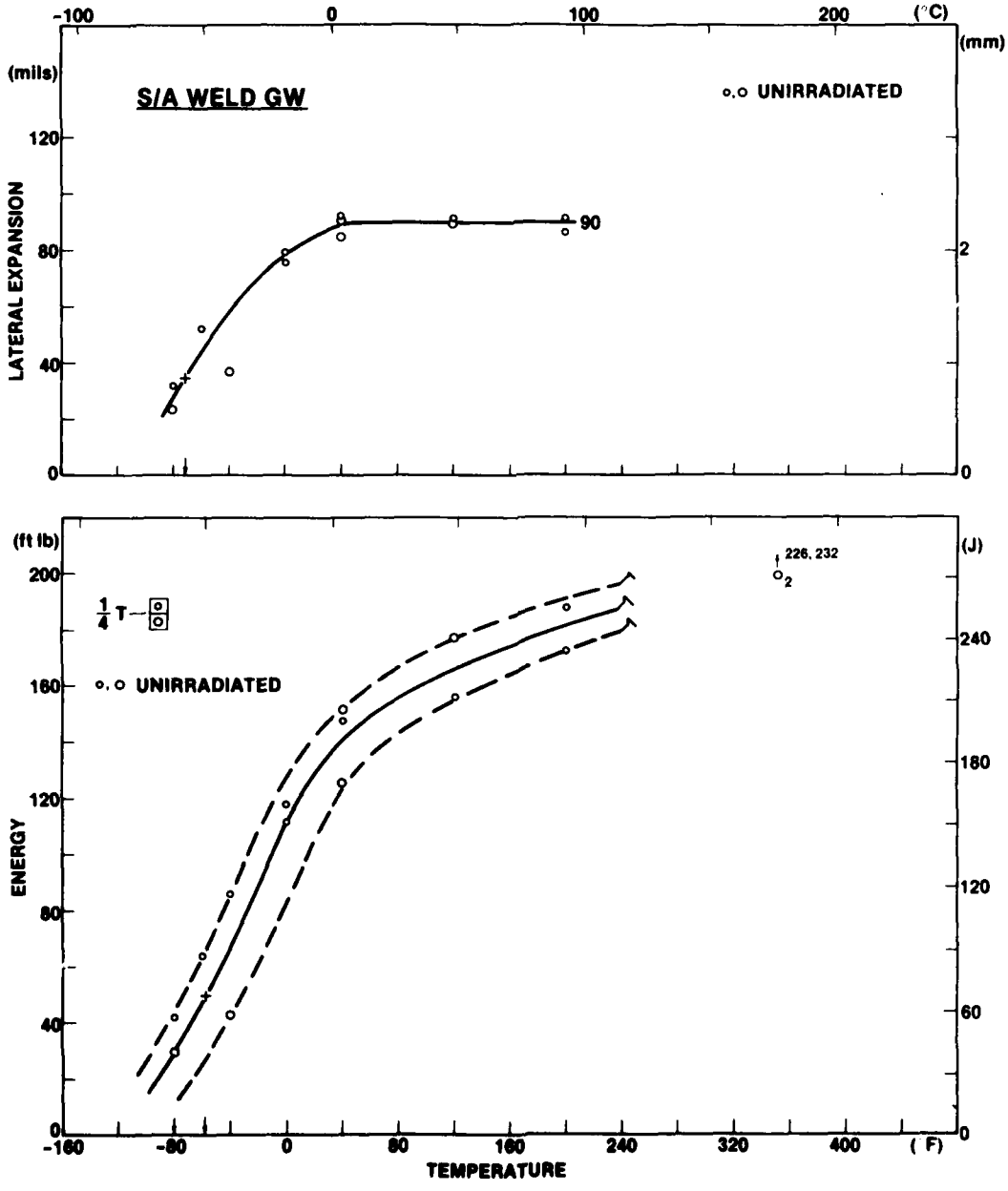

Fig. 31 — Charpy-V notch ductility of the submerged arc (S/A) weld (Code GW) supplied by the FRG to the IWG-RRPC cooperative program

C. Mechanical Properties of LWR-PVI Surveillance Dosimetry Program Steels

J. R. Hawthorne

BACKGROUND

The light water reactor, pressure vessel irradiation (LWR-PVI) surveillance dosimetry program was established by the NRC for improving neutron dosimetry and radiation damage analysis procedures for the more accurate prediction of radiation-induced changes in reactor vessel steel properties. Immediate program objectives are: (1) the development of improved dosimetry and associated damage exposure correlation standards for surveillance, and (2) the performance of supporting validation and calibration experiments in reference, i.e., "benchmark," radiation environments including a spectrum of test reactor and power reactor environments [19]. Although the primary effort is being funded by the NRC, the total program represents a worldwide cooperative research attack on common dosimetry issues.

In reactor surveillance, problems with the measurement of neutron flux and spectrum are generally associated with two aspects of damage analysis. The proper calculation and projection of fluence values for points within the vessel wall forms one problem area. The understanding of relative property change between test and power reactor irradiations comprises the second area. One important part of the LWR-PVI surveillance dosimetry program contributing to both areas of study is the irradiation of metallurgical specimens in a pressure vessel mock-up facility together with extensive dosimetry. The mechanical properties data will serve to validate and calibrate dosimetry and damage analysis techniques and, additionally, will help to refine current mechanical property-neutron exposure correlations and predictive capabilities.

The Naval Research Laboratory (NRL) has participated extensively in the planning for the mechanical properties investigations, and further, as a primary laboratory for the mechanical properties portion of the program investigations, is committed to the testing and analysis of the standard Charpy-V (C_v), compact tension (CT), and tension test specimens from experiments irradiated in the pressure vessel mock-up known as the pool side facility (PSF) [20]. The C_v tests are to be made in the dynamic mode; the CT tests are to be conducted in the static mode. In addition to postirradiation testing, NRL is responsible for the unirradiated condition testing of selected reference correlation materials designated by the NRC. These include the ASTM A302-B reference plate [21], and the A533-B Plate 03 from the NRC HSST Program [22].

PROGRESS

Progress includes: (1) the acquisition of reference materials and the fabrication of requisite specimens for PSF experiments, and (2) the performance of unirradiated condition (control) tests.

Specimen Fabrication

A total of 140 C_v, 30 tensile, 64 0.5T-CT and 30 1T-CT specimens were fabricated from a full thickness section of the A302-B reference plate obtained from NRL stock (Material Code F23). The specimens represent the LT (longitudinal) test orientation and were taken from 1/4 and 3/4 thickness locations within the plate according to NRL cutting plan LFG6678. A total of 64 C_v, 12 tensile, 40 0.5T-CT, and 20 1T-CT specimens were fabricated from three full thickness sections of the A533-B reference plate obtained from ORNL stock (NRL Material Codes 3PS, 3PT, and 3PU). Specimens

were taken from the 1/4 and 3/4 thickness locations in the sections in accordance with NRL cutting plan LFG6878. The specimen test orientation in this case was the TL (transverse) orientation. The C_v and 4.52 mm (0.178 in.) gage diameter tensile specimens were machined to drawing A2389 Mod. 1 and drawing CZS51278, respectively. The 0.5T-CT and 1T-CT specimens were machined to drawing JRH/LFG 61278 (Mods. 1 and 2) and drawing 1000225 (Mods. 1 and 2), respectively, and were fatigue precracked to an a/W ratio (aim) of 0.53 in compliance with requirements of ASTM Standard E399. Specimen blanking and machining drawings are on file at NRL.

Specimen Testing

Charpy-V tests of the unirradiated condition were completed for both reference plates during this reporting period. The tests were conducted using a 298 J (220 ft-lb) capacity Testing Machines, Inc., tester. The same tester will be used for postirradiation evaluations and has demonstrated calibration accuracy with Army Mechanics and Materials Research Center specimen standards. Dynatup equipment and instrumentation were employed to secure applied load vs time of fracture records for the specimens.

Charpy-V results for the A302-B reference plate are given in Fig. 32 and are summarized in Table 12. The data indicate C_v 41 J (30 ft-lb) and C_v 68 J (50 ft-lb) transition temperatures of -4 and 21°C, respectively. Upper shelf behavior begins at about 82°C with an average energy level of 108 J (80 ft-lb). A slight increase in upper shelf level with temperature appears to be a characteristic of this plate. The C_v results for the A533-B reference plate are given in Fig. 33 and are summarized in Table 13. Here, the C_v 41 J and C_v 68 J transition temperatures are -1 and 24°C, respectively. The upper shelf level of this steel based on an average of the data is 150 J (111 ft-lb) and develops at about 116°C.

Preparations are now underway for conducting tensile tests for the reference plates. Data are currently available for other sections of these same plates; however, it is important to the program goals to establish unirradiated condition properties at the same plate location as used for irradiation tests to avoid the introduction of errors. Errors due to across plate property differences can be particularly significant when determining radiation effects at low fluences [23] and for other property correlations planned for the full program.

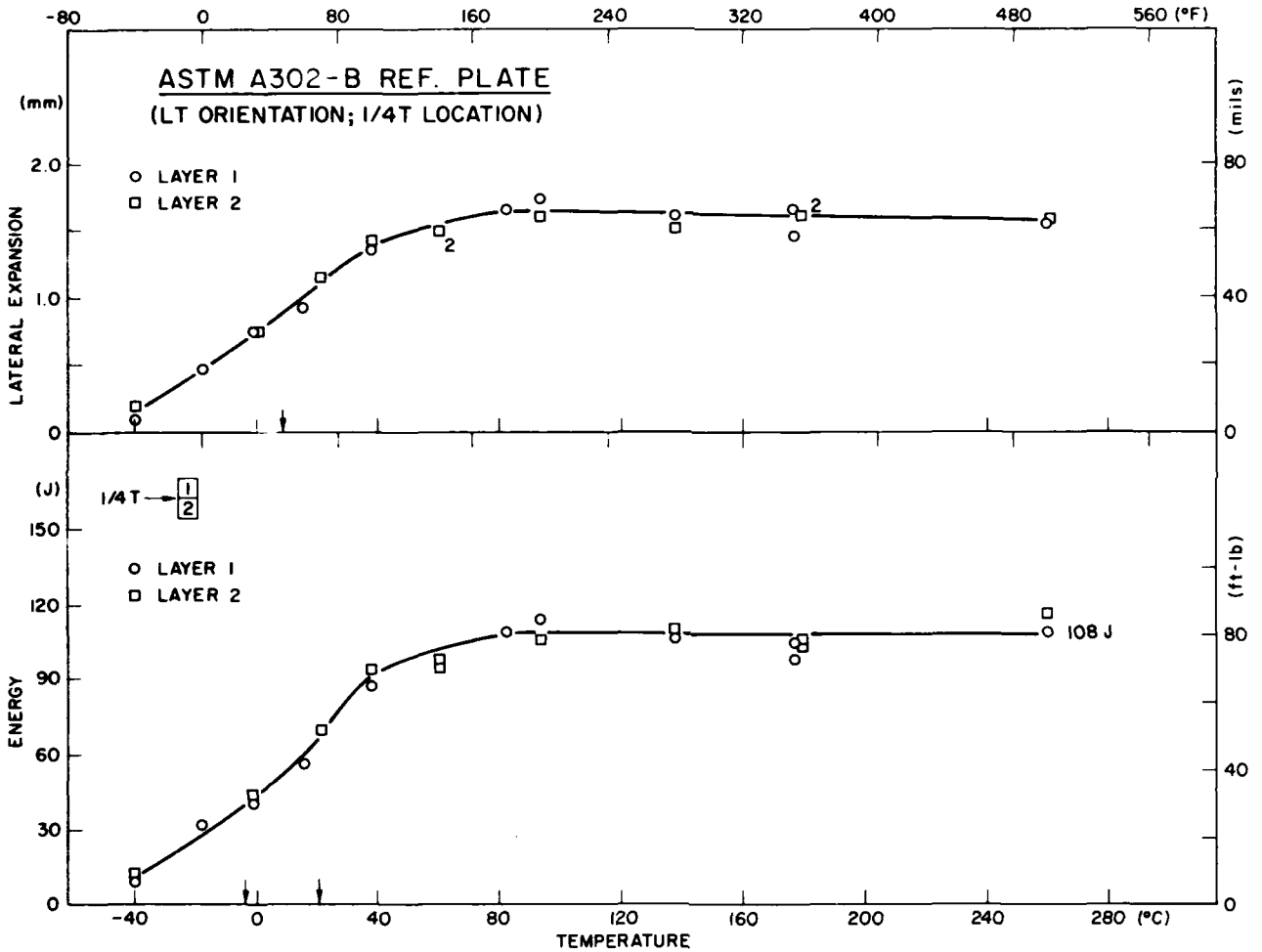

Fig. 32 — Charpy-V notch ductility of section F23 of ASTM A302-B reference plate used for LWR-PVI surveillance dosimetry program. Specimens were removed in two layers spanning the one quarter thickness location.

TABLE 12 -Charpy-V Notch Ductility of ASTM A302-B Reference Plate
(NRL Code F23, LT Orientation, 1/4T Plate Location)

Specimen	°C	°F	Energy J	Energy ft-lb	Lateral Expansion mm	Lateral Expansion mils
(Layer 1)						
6	-40	-40	9	7	.10	4
23	-18	0	33	24	.48	19
43	-1	30	41	30	.76	30
75	16	60	57	42	.94	37
82	38	100	88	65	1.37	54
143	82	180	110	81	1.68	66
89	93	200	115	85	1.75	69
90	138	280	107	79	1.63	64
136	177	350	99	73	1.47	58
83	177	350	106	78	1.68	66
137	260	500	110	81	1.58	62
(Layer 2)						
107	-40	-40	14	10	.20	8
16	-1	30	45	33	.76	30
168	21	70	71	52	1.17	46
68	38	100	95	70	1.45	57
114	60	140	95	70	1.50	59
103	60	140	99	73	1.52	60
48	93	200	107	79	1.63	64
161	138	280	111	82	1.52	60
115	177	350	104	77	1.65	65
100	177	350	107	79	1.63	64
162	260	500	118	87	1.60	63

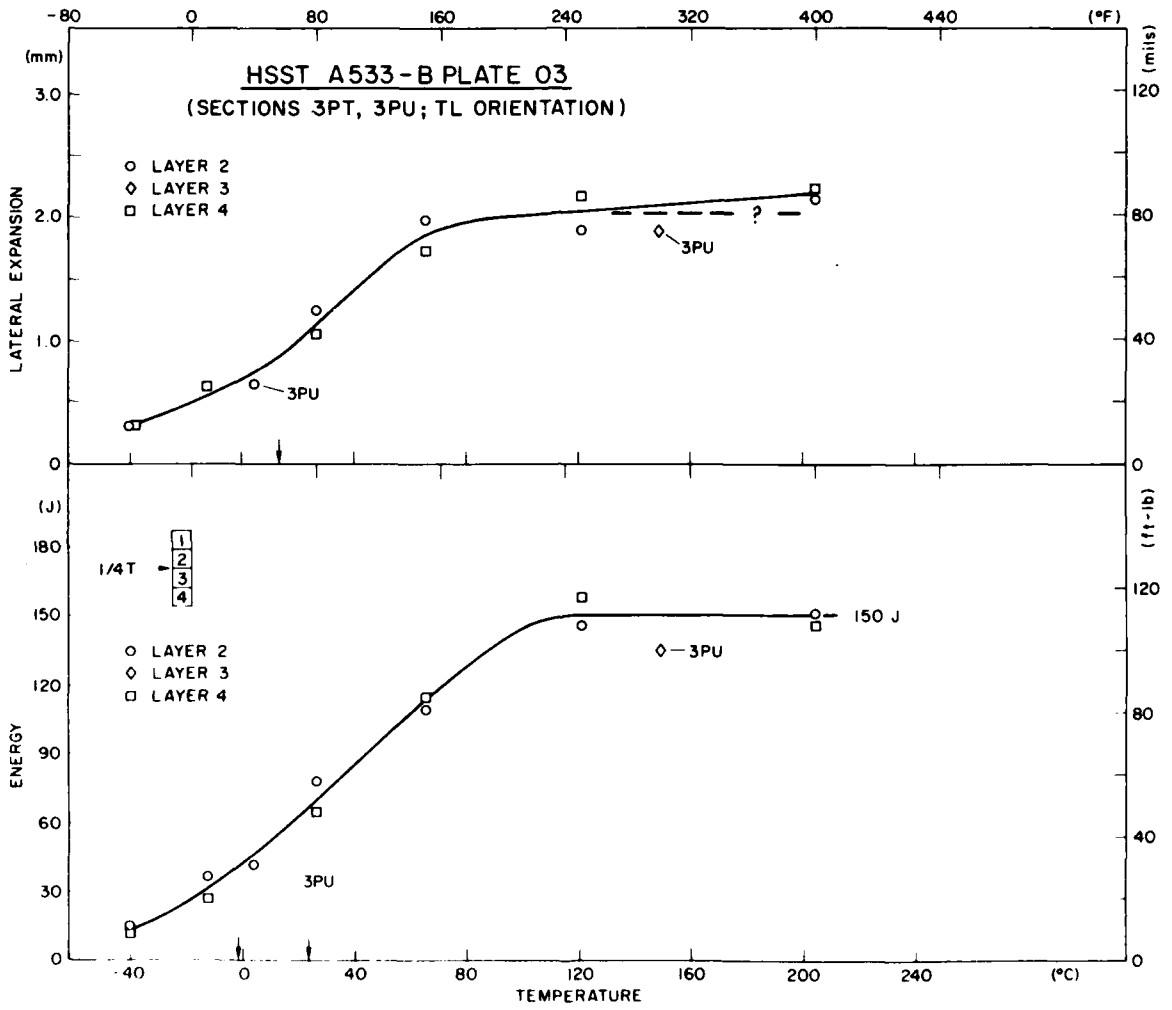

Fig. 33 — Charpy-V notch ductility of two sections of HSST plate 03 used for LWR-PVI surveillance dosimetry program. Specimens were removed in four layers spanning the one quarter thickness location; data for three layers only are shown.

TABLE 13 - Charpy-V Notch Ductility of HSST A533-B Plate 03
(NRL Codes 3PT and 3 PU, TL Orientation, 1/4T Plate Location)

Specimen	°C	°F	Energy J	Energy ft-lb	Lateral Expansion mm	Lateral Expansion mils
(Layer 2)						
16	-40	-40	15	11	.31	12
11	-12	10	37	27	-	
12	27	80	79	58	1.25	49
15	66	150	110	81	1.98	78
13	121	250	146	108	1.91	75
14	204	400	152	112	2.16	85
(Layer 4)						
32	-40	-40	12	9	.31	12
27	-12	10	27	20	.64	25
28	27	80	65	48	1.07	42
31	66	150	115	85	1.73	68
29	121	250	159	117	2.18	86
30	204	400	146	108	2.24	88
(Layer 2)+						
16	4	40	42	31	.64	25
(Layer 3)+						
32	149	300	134	99	1.91	75

*Code 3PT unless noted.
+Code 3 PU

REFERENCES

1. F. J. Loss, Ed., "Structural Integrity of Water Reactor Pressure Boundary Components, Annual Report, Fiscal Year 1979," NUREG/CR-1128, NRL Memorandum Report 4122, Dec. 31, 1979.

2. P. Paris, H. Tada, A. Zahoor, and H. Ernst, "A Treatment of the Subject of Tearing Instability," NUREG 0311, Nuclear Regulatory Commission, Aug. 1977.

3. G. A. Clarke, W. R. Andrews, P. C. Paris, and D. W. Schmidt, "Single Specimen Tests for J_{Ic} Determination," ASTM STP 590, 1976, pp. 27-42.

4. F. J. Loss and G. Angelino, "Elastic-Plastic Characterization of Nuclear Vessel Steels," Proceedings of Intn. Conference on Analytical and Experimental Fracture Mechanics," Rome, Italy, 23-27 June 1980.

5. F. J. Loss, Ed., "Structural Integrity of Water Reactor Pressure Boundary Components, Progress Report Ending 29 Feb 1976," NRL Report 8006, Aug. 26, 1976.

6. J. G. Merkle and H. C. Corten, "A J Integral Analysis for the Compact Specimen, Considering Axial Force as well as Bending Effects," J. Pressure Vessel Tech., Trans. ASME, Nov. 1974, pp. 286-292.

7. G. Gabetta and V. Provenzano, "Fractographic and Microstructural Analysis of Fatigue Specimens of A302 Grade B Steel Tested in Air at Room Temperature," NRL Memorandum Report 4062, Sep. 28, 1979.

8. A. Saxena and S. J. Hudak, "Review and Extension of Compliance Information for Common Crack Growth Specimens," Intn. J. of Fracture, Vol. 14, 1978, pp. 453-468.

9. C. F. Shih, "An Engineering Approach for Examining Crack Growth and Stability in Flawed Structures," Proceedings of CSNI Specialists Meeting on Plastic Tearing Instability, NUREG/CP-0010, Nuclear Regulatory Commission, Jan. 1980.

10. W. H. Cullen, Jr., et al. "Fatigue Crack Growth of A508 Steel in High-Temperature, Pressurized Reactor-Grade Water", NUREG/CR 0969, NRL Memorandum Report 4063, Sep. 1979.

11. Section XI - ASME Boiler and Pressure Vessel Code, Rules for Inservice Inspection of Nuclear Power Plant Components, American Society of Mechanical Engineers, New York, New York 10017, issued annually.

12. W. H. Cullen, Jr., et al. "Evaluation of Critical Factors in Crack Growth Rate Studies" in Structural Integrity of Water Reactor Pressure Boundary Components, Quarterly Progress Report, October-December 1979, NUREG/CR-1268, NRL Memorandum Report 4174, Mar. 1980.

13. W. H. Bamford, D. M. Moon and L. J. Ceschini, "Effects of High Temperature Primary Reactor Water on Fatigue Crack Growth of Reactor Vessel Steels" in HSST Quarterly Report for April-June 1979, ORNL/NUREG/TM-347, Oct. 1979, pp. 9-35.

14. W. H. Cullen, Jr., et al., "Evaluation of Starting ΔK Phenomenon on Cyclic Crack Growth in A508 Pressure Vessel Steels", Report of NRL Progress, Sep. 1978, pp. 4-9.

15. F. J. Loss (Ed.), "Structural Integrity of Water Reactor Pressure Boundary Components," NRL Memorandum Report 3600, Naval Research Laboratory, Sep. 1977.

16. J. R. Hawthorne, H. E. Watson, and F. J. Loss, "Experimental Investigation of Multicycle Irradiation and Annealing Effects on Notch Ductility of A533-B Weld Deposits," in Proceedings, Symposium on Effects of Radiation on Materials, Savannah, Georgia, 3-5 June 1980.

17. F. J. Loss, et al., "J-R Curve Characterization of A533-B Weld Metal With Irradiation and Postirradiation Annealing," in Proceedings, Symposium on Effects of Radiation on Materials, Savannah, Georgia, 3-5 June 1980.

18. "Coordinated Research Programme on Analyses of the Behavior of Advanced Reactor Pressure Vessel Steels Under Neutron Irradiation," Proceedings, IWG-RRPC-78/3, Vienna, Austria, 17-18 Oct. 1977.

19. G. L. Guthrie, E. P. Lippencott, W. N. McElroy and R. Gold, "LWR Pressure Vessel Irradiation Surveillance Dosimetry," NUREG/CR-0038, Nuclear Regulatory Commission, Nov. 1978.

20. Minutes of LWR-PVI Irradiation Surveillance Dosimetry Program: Activities, Status and Scheduling Meeting, 6-8 November 1979, National Bureau of Standards, Gaithersburg, Maryland.

21. J. R. Hawthorne, "Radiation Effects Information Generated on the ASTM Reference Correlation-Monitor Steels," ASTM Data Series 54, American Society for Testing and Materials, 1974.

22. C. E. Childress, "Manual for ASTM A533 Grade B Class 1 Steel (HSST Plate 03) Provided to the International Atomic Energy Agency," ORNL-TM-3193, Oak Ridge National Laboratory, Mar 1971.

23. J. R. Hawthorne, "Notch Ductility Degradation of Low Alloy Steels with Low-to-Intermediate Neutron Fluence Exposures," NUREG/CR-1053, NRL Report 8357, Naval Research Laboratory, Jan. 14, 1980.

END

DATE
FILMED

9-80

DTIC